AJRCMB Articles in Press. Published on 09-May-2014 as 10.1165/rcmb.2013-0471OC

Secreted phosphoprotein 1 (*Spp1*) is a determinant of lung function development in mice

Koustav Ganguly[1,2], Timothy M. Martin[1], Vincent, J Concel[1], Swapna Upadhyay[1,3], Kiflai Bein[1], Kelly A. Brant[1], Leema George[2], Ankita Mitra[2], Tania A. Thimraj[2], James P. Fabisiak[1], Louis J Vuga[4,5], Cheryl Fattman[1], Naftali Kaminski[4,5,6], Holger Schulz[7], George D. Leikauf[1]

[1]Department of Environmental and Occupational Health, Graduate School of Public Health, University of Pittsburgh, Pittsburgh, PA, USA
[2]SRM Research Institute, SRM University, Chennai, Tamil Nadu, 603203 India
[3]Department of Biotechnology, Indian Institute of Technology Madras, Chennai, Tamil Nadu 600036 India
[4]Department of Medicine, University of Pittsburgh, Pittsburgh, PA, USA
[5]Simmons Center for Interstitial Lung Disease, Department of Medicine, University of Pittsburgh, Pittsburgh, PA,USA
[6]Pulmonary, Critical Care and Sleep Medicine, Department of Medicine, Yale School of Medicine, New Haven, CT 06520, USA
[7]Institute of Epidemiology I, Helmholtz Zentrum Munich, German Research Center for Environmental Health, Neuherberg, Munich, D85764 Germany

Correspondence to:
Koustav Ganguly, Ph.D. or George D. Leikauf, Ph.D.
Department of Environmental and Occupational Health
Graduate School of Public Health
University of Pittsburgh
100 Technology Drive, Suite 350
Pittsburgh, PA 15219-3130
Phone: (412) 383-5305
Email: kog8@pitt.edu or gleikauf@pitt.edu

This study was supported by the NIH: (G.D.L): ES015675, HL077763, HL085655, (N.K.): HL084932, HL095397, DST-SERB (K.G.): SB/SO/AS-026/2013

Running Title: SPP1 and lung function development

This manuscript has supplmental material.

Abstract

Secreted phosphoprotein 1 (*Spp1*) is located within quantitative trait loci associated with lung function that was previously identified by contrasting C3H/HeJ and JF1/Msf mouse strains that have extremely divergent lung function. JF1/Msf mice with diminished lung function had reduced lung SPP1 transcript and protein during the peak stage of alveologenesis (postnatal day 14-28) as compared to C3H/HeJ mice. In addition to a previously identified genetic variant that altered runt related transcription factor 2 (RUNX2) binding in the *Spp1* promoter, we identified another promoter variant in a putative RUNX2 binding site that increased the DNA protein binding. SPP1 induced dose dependent MLE-15 cell proliferation. *Spp1*$^{(-/-)}$ mice have decreased specific total lung capacity/body weight, higher specific compliance, and increased mean airspace chord length (L_m) compared to *Spp1*$^{(+/+)}$ mice. Microarray analysis revealed enriched gene ontogeny (GO) categories with numerous genes associated with lung development and/or respiratory disease. IGF1, HHIP, WNT5A, and NOTCH1 transcripts decreased in the lung of P14 *Spp1*$^{(-/-)}$ mice as determined by qRT-PCR analysis. SPP1 promotes pneumocyte growth and mice lacking SPP1 have smaller, more compliant lungs with enlarged airspace (increased L_m). Microarray analysis suggests a dysregulation of key lung developmental transcripts in gene targeted *Spp1*$^{(-/-)}$ mice particularly during the peak phase of alveologenesis. In addition to its known roles in lung disease, this study supports SPP1 as a determinant of lung development in mice.

Word Count: 228 words

Keywords: osteopontin, chronic obstructive pulmonary disease, asthma, emphysema, pulmonary fibrosis

AJRCMB Articles in Press. Published on 09-May-2014 as 10.1165/rcmb.2013-0471OC

CLINICAL RELVANCE

Inappropriate lung development is a risk factor for lower basal pulmonary function as well as defective repair and remodelling processes following lung injury thereby predisposing individuals to asthma, pulmonary fibrosis, and chronic obstructive pulmonary diseases (COPD). This study examines the role of secreted phosphoprotein 1 (SPP1), a protein previously associated with pulmonary fibrosis and COPD, in lung development in mice. A mouse strain with decreased lung function has decreased lung SPP1 during postnatal alveologenesis. Mice have a genetic variant in the *Spp1* promoter that is near a similar transcription factor binding site that is variant in humans. *Spp1*-deficent mice have smaller alveoli and decreased lung function.

Introduction

Chronic lung diseases are leading causes of death worldwide (1). Impaired lung development is associated with lower basal pulmonary function as well as defective repair and remodelling processes following lung injury thereby predisposing individuals to chronic lung disease (2-7). Recently, the molecular pathways of lung development have been described (8, 9) and genes associated with lung function have been identified by genome wide association studies (GWAS) (10-14). However, genetic variants in significant loci explained only a modest portion of the variance for forced expiratory volume in 1s, (FEV1) or FEV1/ forced vital capacity (FEV1/FVC) (15, 16). Thus, much of the heritability remains unexplained by individual variants identified in GWAS, which is common with complex phenotypes (17, 18). In addition, the functional consequence of these genes and the downstream effectors of lung function have not been fully explored.

To further address the genetics of lung development and function, we utilized a diverse panel of inbred mice (19), a model organism with an extensive genetic architecture. We previously identified several quantitative trait loci (QTL) for lung function in mice by contrasting two strains (C3H/HeJ vs. JF1/Msf) with extremely divergent pulmonary function, e.g., the total lung capacity (TLC) of C3H/HeJ = 1443 $\pm$ 30 μL and JF1/Msf = 874 $\pm$ 17 μL (19, 20). In the past, we identified candidate genes located in QTLs on various regions of mouse chromosome 5 that include superoxide dismutase 3, extracellular (*Sod3*) (21, 22) and c-Kit oncogene (*Kit*) (23) as determinants of dead space volume (V_{DS}) and lung compliance (C_L), respectively. In children, we found that *SOD3* single-nucleotide polymorphisms (SNPs) were associated with decreased FEV1 and maximal expiratory flow at 25% volume (22). In adults, *SOD3* SNPs have been associated with lower lung function (24, 25) and increased risk of developing chronic obstructive pulmonary disease (COPD) (26). These findings support the rapid identification of candidate genes in mice that can later be tested in human populations.

In this study we sought to determine whether secreted phosphoprotein 1 (*Spp1* a.k.a. osteopontin) is a functional candidate gene for lung development in mice. *Spp1* is located within another QTL associated with lung function on mouse chromosome 5 bounded by markers *D5Mit20* to *D5Mit403* (97.8-106.2Mbp) (20, 21), which is syntenic to human chromosome 4 (81.8-90.2Mbp). Previously, SPP1 has been associated with chronic lung diseases including pulmonary fibrosis (27), and COPD (28). A ~44KDa glycosylated phosphoprotein, SPP1 is commonly found in adhesive bone matrix protein. It is also

AJRCMB Articles in Press. Published on 09-May-2014 as 10.1165/rcmb.2013-0471OC

recognized as a key cytokine involved in immune cell recruitment and type-1 (Th1) cytokine expression at sites of inflammation (29, 30) and a mediator of tissue repair and remodelling (31, 32). Past studies on SPP1 focused mainly on its association with bone metabolism, inflammation, and cancer; however, the role of SPP1 in lung development is unknown.

In this study we examined lung SPP1 expression in mice and found strain specific differences during development. Previously, Shen and Christakos (33) reported that the mouse *Spp1* promoter contained functional runt related transcription factor 2 (RUNX2) (-136 to -130 bp from the transcription start site), and vitamin D response element (VDR) (-757 to -743) binding sites that cooperatively regulate transcriptional activation by 1,25-dihydroxyvitamin D_3 [1,25(OH) D_3]. In cells transfected with hes family bHLH transcription factor 1 (aka hairy and enhancer of split 1, HES1), basal and 1,25(OH) D_3-induced SPP1 transcripts increased indicating involvement of the NOTCH1 pathway. Subsequently, Sowa et al. (34) PCR amplified and sequenced the mouse *Spp1* promoter in the C3H/HeJ and compared this sequence with the promoter of the reference C57BL/6J strain. One variant, a 13-bp insertion (rs234069704) at position -130 (5'- TTTTTTTTTTTTA -3'), was located at the 3' end of the RUNX2 binding site. This insertion increased transcriptional responsiveness to RUNX2 in the C3H/HeJ promoter as compared to that of the C57BL/6J promoter. Based on these studies we further examined *Spp1* promoter polymorphisms in mice.

Materials and Methods

Detailed methods are contained in the online supplement. Briefly, studies were approved by the Bavarian Animal Research Authority and by the IACUC of the University of Pittsburgh. Mice {C3H/HeJ, JF1/Msf, *Spp1*$^{(-/-)}$ [B6.129S6(Cg)-Spp1^{tm1Blh}/J], and *Spp1*$^{(+/+)}$ (C57BL/6J)} were purchased from Jackson Laboratory. Quantitative real time-polymerase chain reaction (qRT-PCR) was used to determine lung SPP1 transcripts using the $2^{-\Delta\Delta CT}$ method normalized to actin, beta (ACTB) as described previously (21). ELISA was used to determine lung SPP1 protein levels. Mouse lung MLE-15 cells are an immortalized cell line obtained from transgenic mice containing the simian virus 40 large T antigen under the transcriptional control of the human surfactant protein C promoter (35, 36). To measure the effect of SPP1 on cell proliferation, sub-confluent MLE15 cells were serum deprived 24 h, 0 (control), or 1-4 μg/ml SPP1 was added to the culture medium, and growth was assessed at 48h using an alamarBlue cell viability assay. To

assess the consequences of SNPs on the binding of nuclear protein, PCR amplification of the *Spp1* promoter region was performed using genomic DNA from C3H/HeJ and JF1/Msf mice and sequenced in forward and reverse directions (Sequiserve, Vaterstetten, Germany). Two of the identified SNPs were used for an electrophoretic mobility shift assay (EMSA) performed using nuclear protein extracts from MLE15 cells. Double-stranded 25mer oligonucleotides were prepared by annealing complementary synthetic oligonucleotides corresponding to the *Spp1* promoter region containing G/T rs264140167 or A/G rs47003578 alleles. Lung function was measured in 27 strains of inbred mice (females, 13-17 wk; n = 252 mice), and $Spp1^{(-/-)}$ and strain, sex, and age-matched control $Spp1^{(+/+)}$ mice as described (19, 20, 37). To assess lung morphology, mean chord length (L_m) was measured from images to estimate the alveolar size of $Spp1^{(-/-)}$ mice and compared to strain, sex and age-matched $Spp1^{(+/+)}$ as descibed (22). For immnunohistochemical localization, $Spp1^{(+/+)}$ lung sections were stained using a goat anti-mouse SPP1 antibody (AF-808 R&D Systems Inc.) and biotinylated horse-anti-goat secondary antibody (1:200 dilution, Vector Laboratories Inc). Lung transcript levels were measured by microarray (Whole Mouse Genome Kit 4x44K, Agilent Technologies) comparing postnatal day 14 (P14) $Spp1^{(-/-)}$ with P14 $Spp1^{(+/+)}$ and P28 $Spp1^{(-/-)}$ with P28 $Spp1^{(+/+)}$ mice. Postnatal days 14 and 28 were chosen based on reduced SPP1 transcript expression pattern in JF1/Msf lungs compared to C3H/HeJ during peak phase of alveologenesis (P14) and completion of alveologenesis (P28). In addition, insulin-like growth factor 1 (IGF1), wingless-related MMTV integration site 5A (WNT5A), Hedgehog-interacting protein (HHIP), notch 1 (NOTCH1), CD44 antigen (CD44) transcripts were assessed by qRT-PCR using lung RNA from P14 or P28 $Spp1^{(-/-)}$, or P14 or P28 $Spp1^{(+/+)}$ mice. Data are presented as mean values of n observations ± the standard error (SE). Group comparisons were performed using analysis of variance (ANOVA) and all pairwise comparisons procedure (Holm-Sidak method) (Sigma Plot 11.0 software). Significant differences in transcript levels for the microarray data were analyzed using ANOVA (Partek Genomics Suite).

Results

Lung SPP1 transcript and protein expression: Lung SPP1 transcripts decreased in JF1/Msf mice as compared to C3H/HeJ mice during various stages of postnatal lung development between postnatal days (P)14-P70 (Figure 1A). At P7, lung SPP1 transcripts in JF1/Msf mice were not significantly different than in C3H/HeJ mice. However, at P14 and onward, lung SPP1 transcripts decreased in JF1/Msf as compared to

AJRCMB Articles in Press. Published on 09-May-2014 as 10.1165/rcmb.2013-0471OC

C3H/HeJ mice. At P28, lung SPP1 protein decreased in JF1/Msf as compared to C3H/HeJ mice (Figure 1B).

Spp1 promoter analysis: The mouse *Spp1* promoter contained functional RUNX2 binding site (-136 to -130) (33). A 13-bp insertion (rs234069704) at position -130 (5'- TTTTTTTTTTTTA -3') was located at the 3' end of this binding site that increases transcriptional responsiveness to RUNX2 in the C3H/HeJ promoter as compared to that of the C57BL/6J promoter (34). To further analyse the mouse *Spp1* promoter, ~700-bp fragments 5' from the transcription start site of the mouse *Spp1* gene was PCR amplified using the JF1/Msf or C3H/HeJ DNA as a template and sequenced. These sequences were aligned to the reference sequence (obtained from C57BL/6J) (Supplemental Figure S1) and 6 genetic variants [4 single nucleotide polymorphisms (SNPs) and 2 insertions] were identified that differed between JF1/Msf and C3H/HeJ mice (Supplement Table S1). Like the reference C57BL/6J, the JF1/Msf promoter lacks the 13-bp insertion rs234069704. The variation in sequence was then analysed using Matinspector (38) to identify which of the other 4 genetic variants could alter putative transcriptional binding sites. Two of the identified SNPs at position -158 (rs264140167) and -198 (rs47003578) could alter putative binding sites.

Sequence information of these 2 SNPs was used to generate 25-mer biotinylated oligonucleotide probes for EMSA of nuclear protein extract prepared from mouse lung epithelial cells (MLE-15). SNP rs264140167 (-158 nucleotides from the transcription start site) in the *Spp1* promoter region alters the nuclear protein-target DNA binding capacity. The 25-mer probes (-144bp to -168bp) containing C3H/HeJ T allele in the middle of the biotinylated oligonucleotide increased the DNA protein binding, i.e. the C3H/HeJ T allele formed slow migrating complexes and enhanced the intensity of a faster migrating complex compared to the JF1/Msf G allele (Figure 2). The C3H/HeJ T allele forms an additional putative RUNX2 binding site not present in the JF1/Msf G allele. No difference in protein binding was noted in the EMSA when probes were generated from the rs47003578 SNP (JF1/Msf G allele vs C3H/HeJ A allele), which is located -198 nucleotides from the transcription start site (Supplemental Figure S2).

We examined the lung functions of 36 inbred strains of mice to determine the possible functional consequence of rs47003578 SNP (JF1/Msf G allele vs C3H/HeJ A allele). This include 9 strain previously phenotyped (19, 20), and 27 additional mouse strains (Table 1). Mice with JF1/Msf allele had decreased TLC (G allele = 1144 ± 13 vs. T allele = 1205 ± 25 µl, n = 345 mice), decreased specific TLC/body weight

(TLC/BW) (G allele = 54 ± 1 vs. T allele = 57 ± 1 µl/g, n = 369 mice), and increased specific compliance (sC_L: C_L/TLC) (G allele = 58 ± 1 vs. T allele = 54 ± 1 µl/cmH_2O/ml n = 354 mice) (n = 7-15 mice/strain, 12-14 wk). These differences are approximately 11%, 17%, and 21%, respectively, of the phenotypic difference we have previously observed in the extremely divergent mouse strains (19, 20). Body weight (G allele = 22.5 ± 0.4 vs. T allele = 22.6 ± 0.6 g n = 382 mice) and other lung function measurements (e.g., dead space volume)) were not statistically different between genotypes.

SPP1 induces mouse pneumocyte growth: Considering that lung SPP1 transcripts and protein decreased in JF1/Msf mice during the peak stage of alveologenesis, we investigated whether SPP1 protein could stimulate the growth of mouse lung epithelial cells. MLE-15 cell proliferation increased 48h after treatment with 2 µg/ml and 4µg/ml SPP1 (Supplemental Figure S3).

Lung function of $Spp1^{(-/-)}$ mice: Analysis of lung function revealed that $Spp1^{(-/-)}$ had decreased TLC ($Spp1^{(-/-)}$ = 1034 ± 25 vs. $Spp1^{(+/+)}$ = 1220 ± 22µl), decreased specific TLC/body weight (TLC/BW) ($Spp1^{(-/-)}$ = 48 ± 1 vs.$Spp1^{(+/+)}$ = 58 ± 1µl/g), and increased sC_L ($Spp1^{(-/-)}$ = 54 ± 1 vs. $Spp1^{(+/+)}$ = 47 ± 1µl/cmH_2O/ml) (n = 8 mice/strain, 12-14 wk) (Figure 3). These differences are approximately 33%, 38%, and 16%, respectively, of the phenotypic difference we have previously observed in the extremely divergent mouse strains (20). Other lung function measurements (including dead space volume and diffusion capacity/TLC) and BW ($Spp1^{(-/-)}$ = 21.5 ±0 .9 vs.$Spp1^{(+/+)}$ = 21.0 ± 0.8g) were not statistically different between $Spp1^{(-/-)}$ and $Spp1^{(+/+)}$ mice.

Lung Morphometry and SPP1 immunohistochemical location: Increased airspace chord length (L_m) indicates decreased alveolar surface area. The mean chord length in $Spp1^{(-/-)}$ increased as compared to $Spp1^{(+/+)}$ mice (Figure 4). This was detected in P28 mice when lung development is just completed and is indicative of impaired alveologenesis. Immunohistiological analysis localized SPP1 protein to the bronchial epithelium, alveolar macrophage, and weakly to the alveolar type II cell in adult $Spp1^{(+/+)}$ mice (Supplemental Figure S4)

Transcriptomic Analysis: To assess the lung transcriptomic profile during P14 (peak alveologenesis phase) and P28 (completion of alveologenesis and lung development), microarray analysis was performed with mRNA isolated from $Spp1^{(-/-)}$ and $Spp1^{(+/+)}$ mouse lung. P14 and P28 were chosen based on reduced SPP1 transcript expression pattern in JF1/Msf lungs compared to C3H/HeJ. Initially, we examined the transcripts that were increased or decreased at P14 or P28 (n=7384). These transcripts were significantly

AJRCMB Articles in Press. Published on 09-May-2014 as 10.1165/rcmb.2013-0471OC

enriched in genes associated with gene onotogy category GO:0030324 lung development (n = 132 significant of 387 in the category, p = 1.0E-08) (Figure 5). These 132 transcripts grouped into 4 clusters including transcripts that: (A) decreased at P14 and P28, (B) increased at P14 and decreased at P28, (C) decreased at P14 and increased at P28, or (D) increased at P14 and P28. These clusters were analyzed for enrichment in transcripts associated with canonical pathways using Ingenuity Pathway Analysis. The top pathway for each cluster included: (A) retinoic acid receptor (RAR) activation (p =1.7E-06), (B) aryl hydrocarbon receptor signaling (p = 1.4E-04), (C) notch signaling (p = 7.8E-04), and (D) bone morphogenetic protein (BMP) signaling pathway (p = 1.8E-0.8), and fibroblast growth factor (FGF) signaling (p = 1.5E-0.6), respectively.

Next, transcripts ≥ 1.5-fold increased or ≤ 1.5-fold decreased in *Spp1*$^{(-/-)}$ lung as compared to *Spp1*$^{(+/+)}$ were analyzed for enriched pathways using Database for Annotation, Visualization, and Integrated Discovery (DAVID) (39, 40). The enriched categories of Gene Ontogeny (GO) molecular function, GO biological process, GO cell component, and Kyoto Encyclopedia of Genes and Genomes (KEGG) pathways were determined. Ten transcripts with the greatest difference between strains at age P14 or P28 in each of these GO/KEGG categories are listed in Tables 2-5.

The GO/KEGG categories at P14 containing increased transcripts (n = 738 transcripts with unique Entrez Gene ID) in *Spp1*$^{(-/-)}$ mouse lung were protein tyrosine kinase activity, blood vessel morphogenesis, and cell projection (Table 2). Several genes or gene products in these pathways have been associated with abnormal lung development or lung disease (e.g., asthma, or COPD). Noteworthy transcripts in these categories/pathway included fibroblast growth factor receptor 3 (FGFR3) (41), hypoxia inducible factor 1, alpha subunit (HIF1A) (42), intelectin 1 (ITLN1) (43,44), and heme oxygenase 1 (HMOX1) (45,46).

The GO/KEGG categories at P14 containing decreased transcripts (n = 388) in *Spp1*$^{(-/-)}$ mouse lung were peptidase activity, response to wounding, extracellular space, cytokine-cytokine receptor interaction (Table 3). Noteworthy transcripts in these categories/pathway included matrix metalloproteinase 25 (MMP25 aka MT-MMP6) (47), thrombospondin 1 (THBS1) (48, 49), toll-like receptor 1 (TLR1) (50,51), TLR5 (52), chitinase 3-like 1 (CHIL3L1) (53,54), and interleukin 12b (IL12B) (55, 56).

The GO/KEGG categories at P28 containing increased transcripts (n = 1436) in *Spp1*$^{(-/-)}$ mouse lung were zinc ion binding, regulation of transcription, microtubule cytoskeleton and cell cycle (Table 4). Noteworthy transcripts in these categories/pathway included forkhead box P2 (FOXP2) (57), midline 1

(MID1) (58), metal response element binding transcription factor 1 (MTF1) (59), SRY-box containing gene 9 (SOX9) (60), SOX5 (61), nuclear factor I/A (NFIA) (62), sperm associated antigen 17 (SPAG17) (63).

The GO/KEGG categories at P28 containing decreased transcripts (n = 1161) in *Spp1*$^{(-/-)}$ mouse lung were protein kinase activity, protein kinase cascade, cell-cell junction, and tight junction (Table 5). Noteworthy transcripts in these categories/pathway included casein kinase 1, epsilon (CSNK1E) (64), mitogen-activated protein kinase 6 (MAPK6 aka ERK3) (65), mechanistic target of rapamycin (serine/threonine kinase) (MTOR) (66), oncostatin M (OSM) (67, 68), TLR6 (69), mucin 20 (MUC20) (70,71), MAD homolog 1 (SMAD1) (72,73), FGFR3, protein phosphatase 2 (formerly 2A), catalytic subunit, alpha isoform (PPP2CA) (74,75), claudin 3 (CLDN3), CLDN4, CLDN5, CLDN7 (76-78) and lethal giant larvae homolog 2 (Drosphila) (LLGL2) (79, 80).

To further assess transcripts associated with lung development, transcripts encoding insulin-like growth factor 1 (IGF1), wingless-related MMTV integration site 5A (WNT5A), hedgehog interacting protein (HHIP), notch 1 (NOTCH1), and CD44 antigen (CD44) were assessed by qRT-PCR. As compared to P14 *Spp1*$^{(+/+)}$ mice, lung IGF1, WNT5A, HHIP, and NOTCH1 transcripts decreased in P14 *Spp1*$^{(-/-)}$ mice (Figure 6A). At P28, only HHIP was decreased in *Spp1*$^{(-/-)}$ compared to *Spp1*$^{(+/+)}$ mouse lung (Figure 6A).

Discussion

Rapid identification of functional candidate genes in mice has been valuable in providing insights into human lung development. In this study, we assessed the functionality of *Spp1* located within another QTL for lung function for its plausible role as a pulmonary function determinant in mice.

Mammalian lung development is a precisely orchestrated process that involves lung airway branching morphogenesis and alveolarization along with angiogenesis and vasculogenesis during embryonic and postnatal periods (81). Severe impairments during any developmental stage can result in bronchopulmonary dysplasia, neonatal respiratory failure, and death (82). However mild structural or functional defects due to aberrant lung development (83) may increase susceptibility to subsequent respiratory diseases (COPD, cystic fibrosis, or asthma) that may be clinically detectable only during childhood or later in life through pulmonary function testing (84-87). Therefore it is important to detect genetic abnormalities that can impact early fetal and postnatal lung development, and postnatal lung growth and maturation as well as lung injury, repair and remodeling processes (84-90).

AJRCMB Articles in Press. Published on 09-May-2014 as 10.1165/rcmb.2013-0471OC

In mice, alveolarization takes place between postnatal days P5-P30 and is controlled by finely integrated and mutually regulated networks of transcriptional factors, growth factors, matrix components, and physical forces (9, 89-92). Factors that adversely affect the developing lung include premature birth, oxygen exposure, early corticosteroidal exposure, dysregualated growth factor (viz. IGF, WNT, NOTCH, BMP/TGFB, FGF, PDGF, VEGFA) signaling, and abnormal regulation or injury of the pulmonary capillary vasculature. Individually and cumulatively these factors can result in hypoplasia of the alveolar epithelial surface with a resulting deficiency in pulmonary function (e.g., decreased TLC or increased C_L).

As compared to C3H/HeJ mice, lung SPP1 transcript decreased in JF1/Msf mice, a strain with decreased lung function. This decrease was noted P14 onward which is the peak phase of alveologenesis in mice. Alveolization takes place by the process of septation of primitive saccules into smaller units during late gestation in humans and postnatally in mice. During this period secondary crests develop and extend to form alveoli resulting in increased surface area for gaseous exchange. Alveolization defects result in large alveoli, reminiscent of the abnormality found in emphysema but with less overt destruction. Indicative of impaired alveologeneis, *Spp1*$^{(-/-)}$ mice had increased alveolar size (L_m) that was detectable as early as 4 weeks of age when the process is just completed. Increased alveolar size also implicates reduced alveolar surface area ($S = 4V/L_m$) for gas exchange (93). At around 4 weeks of age the lung development is completed and it assumes the structure of an adolescent lung. Thus, P28 is an important screening stage for evaluating postnatal lung development (21).

Several genetic variants in the *Spp1* proximal promoter differ between C3H/HeJ and JF1/Msf mice. Previously, Sowa et al. (34) identified a 13-bp insertion (rs234069704) at position -130 located at the 3' end of the RUNX2 binding site. This insertion increased transcriptional responsiveness to RUNX2 in the C3H/HeJ promoter as compared to that of the C57BL/6J promoter. Because JF1/Msf mice, similar to C57BL/6J mice, lack the poly-T insertions, C3H/HeJ *Spp1* promoter would also be more responsive to RUNX2 than JF1/Msf promoter. In addition, we examined whether SNPs at position -158 (rs264140167) or -198 (rs47003578) could alter putative binding sites. The C3H/HeJ T rs264140167 allele at -158 in the *Spp1* promoter enhanced nuclear protein-target DNA binding capacity. The C3H/HeJ T allele forms an additional putative RUNX2 binding site not present in the JF1/Msf G allele.

Several variants in the human *SPP1* promoter have been identified and are functional. For example, variants at -66 (rs28357094), -156 (rs11439060), and -443 (rs11730582) bp from the

transcriptional start site can modify activation by Sp1 transcription factor (SP1), RUNX2, and v-myb avian myeloblastosis viral oncogene homolog (MYB), respectively (94, 95). The -156 bp rs11439060 variant is an insertion (−/G), which provides a functional RUNX2 binding site, and is near the -158 SNP in the mouse genome, which also provides a putative RUNX2 binding site in C3H/HeJ mice (Supplemental Figure S5). Human promoter SNPs also have been reported as autoimmune risk variants for systemic lupus erythematosus (96,97), systemic sclerosis (98), inflammatory bowel disease (99), and rheumatoid arthritis (100). RUNX2-mediated *SPP1* promoter activity can be inhibited by histone deacetylase 1 (101), and RUNX transcription factors have been associated with increased risk of asthma in children with in utero smoke exposure (102, 103).

Similar to what we have reported previously with primary human normal lung fibroblast and A549 lung epithelial cell line (27), SPP1 induced mouse MLE-15 cell proliferation. SPP1 also alters fibroblast migration (27) further supporting its likely role in lung development. The smaller TLC and higher C_L in *Spp1*$^{(-/-)}$ mice could be a result of impaired alveologenesis. Inasmuch as SPP1 can influence the proliferation of type II-like epithelial cells and lung fibroblasts, the altered lung function in *Spp1*$^{(-/-)}$ mice may be due to increased alveoloar size or diminished tissue elastic recoil of the lungs. Therefore impaired alveologenesis could explain the decreased TLC and increased C_L observed in SPP1 deficient mice.

Lung microarray analysis revealed numerous differences in transcripts critical to lung development in *Spp1*$^{(-/-)}$ mice as compared to strain-matched control mice. GO categories of molecular function, biological process, and cell component, and KEGG pathways contained transcripts associated with lung development (P14 increased FGFR3, HIF1A; P14 decreased THBS1; P28 increased FOXP2, MTF1, SOX5, SOX9, NFIA, and SPAG17; P28 decreased CSNK1E, MAPK6, SMAD1, FGFR3, PPP2CA, CLDN3, CLDN4, CLDN5, CLDN7 LLGL2) or lung diseases including asthma (P14 increased ITLN1; P14 decreased CHIL3L1, IL12B; P28 increased MID1; P28 decreased MTOR, TLR6, PPP2CA) and COPD (P14 increased HMOX1, P14 decreased MMP25; P28 increased SOX5). These altered transcripts suggest that SPP1 interacts with a wide range of proteins that regulate normal development and also supports the hypothesis that abnormal development is a risk factor for chronic respiratory diseases.

In addition, lung IGF1, HHIP, WNT5A, and NOTCH1 transcripts decreased in P14 Spp1$^{(-/-)}$ mice as determined by qRT-PCR analysis. These transcripts encoded proteins that formed an interactive network that included interactions of SPP1 with IGF1, RUNX2, CD44, FGF2, and integrin alpha V, (ITGAV) (Figure

AJRCMB Articles in Press. Published on 09-May-2014 as 10.1165/rcmb.2013-0471OC

6B). Other proteins were required to include HHIP, WNT5A, and NOTCH1 in the interactome that includes SPP1, suggesting that SPP1 is associated with these transcripts through indirect interactions. In addition, the validated transcripts encode proteins that have key roles in the other regulatory networks that control lung development. In mice, IGF1 regulates airspace formation by promoting an elastogenic lineage in undifferentiated mesenchymal cells (104) and is critical for lung development (105).

HHIP regulates the hedgehog (HH) pathway implicated in development and repair in multiple tissues (106). Gene-targeted HHIP deficient mice display defective airway branching morphogenesis and lung hypoplasia that results in death due to respiratory failure at birth (107). In humans, SNPs located near *HHIP* have been associated with lung development and growth (108) and COPD (10-16, 107-109).

In mice, disruption of *Wnt5a* results in distinct truncation of the trachea and over expansion of the distal respiratory airways (112) whereas over expression of WNT5A interferes with epithelial-mesenchymal crosstalk resulting in reduced airway branching and dilated distal airways (113). In addition, HH and FGF signalling were altered in WNT5A overexpressing mice (113) clearly indicating its role in lung development.

Lastly, NOTCH signalling is critical for normal balance of differentiated cell fates in the airway epithelium (114-115). Transgenic mice expressing a constitutively activated NOTCH1 in the lung epithelium have fewer ciliated cells and more mucin producing cells, suggesting its role in the lineage determination of secretory or nonsecretory cells (116-117). The NOTCH1 pathway has been implicated in SPP1 transcription in HES1 transfected cells, and can be inhibited by AML-1/ETO, an inhibitor of RUNX2 (33).

To summarize, mice with decreased SPP1 have smaller but more compliant lungs, which is likely due to impaired alveologenesis. This is accompanied by altered expression patterns of key lung developmental transcripts in P14 *Spp1*$^{(-/-)}$ mice (during peak alveologenesis phase) and increased alveolar airspace detectable in P28 *Spp1*$^{(-/-)}$ mice (when alveologenesis is nearly complete). Together, these findings support a key role for SPP1 in lung development, which adds to its known role in chronic lung disease.

Author Contributions: KG, HS, NK and GDL conceived the project and designed the experiments. KG, TMM, VJC, SU, KB, KAB, and LJV performed the experiments. KG, HS, NK, GDL, JPF, LG, AM, TAT, and CF analyzed the data. KG, LG, HS and GDL wrote the manuscript.

Acknowledgement: This study was supported by the NIH: (G.D.L): ES015675, HL077763, HL085655, (N.K.): HL084932, HL095397, DST-SERB (K.G.): SB/SO/AS-026/2013; (S.U.) CSIR-SRA (13-8553A)-2012/POOL

AJRCMB Articles in Press. Published on 09-May-2014 as 10.1165/rcmb.2013-0471OC

References

1. Mathers CD, Loncar D. Projections of global mortality and burden of disease from 2002 to 2030. *PLoS Med* 2006;3:e442.

2. Burrows B, Knudson RJ, Lebowitz MD. The relationship of childhood respiratory illness to adult obstructive airway disease. *Am Rev Respir Dis* 1977;115:751-760.

3. Strachan D. Ventilatory function, height, and mortality among lifelong non-smokers. *J Epidemiol Community Health* 1992;46:66-70.

4. Engstrom G, Hedblad B, Janzon L. Reduced lung function predicts increased fatality in future cardiac events. A population-based study. *J Intern Med* 2006;260:560-567.

5. Bridevaux P, Gerbase M, Probst-Hensch N, Schindler C, Gaspoz J, Rochat T. Long-term decline in lung function, utilisation of care and quality of life in modified gold stage 1 copd. *Thorax* 2008;63:768-774.

6. Hirschhorn JN. Genomewide association studies--illuminating biologic pathways. *N Engl J Med* 2009;360:1699-1701.

7. Weiss ST. Lung function and airway diseases. *Nat Genet* 2010;42:14-16.

8. Beers MF, Morrisey EE. The three R's of lung health and disease: repair, remodeling, and regeneration. *J Clin Invest* 2011;121:2065-2073.

9. Morrisey EE, Cardoso WV, Lane RH, Rabinovitch M, Abman SH, Ai X, Albertine KH, Bland RD, Chapman HA, Checkley W, Epstein JA, Kintner CR, Kumar M, Minoo P, Mariani TJ, McDonald DM, Mukouyama YS, Prince LS, Reese J, Rossant J, Shi W, Sun X, Werb Z, Whitsett JA, Gail D, Blaisdell CJ, Lin QS. Molecular determinants of lung development. *Ann Am Thorac Soc* 2013;10:S12-S16.

10. Wilk JB, Chen TH, Gottlieb DJ, Walter RE, Nagle MW, Brandler BJ, Myers RH, Borecki IB, Silverman EK, Weiss ST, O'Connor GT. A genome-wide association study of pulmonary function measures in the framingham heart study. *PLoS Genet* 2009;5:e1000429.

11. Repapi E, Sayers I, Wain LV, Burton PR, Johnson T, Obeidat M, Zhao JH, Ramasamy A, Zhai G, Vitart V, Huffman JE, Igl W, Albrecht E, Deloukas P, Henderson J, Granell R, McArdle WL, Rudnicka AR, Barroso I, Loos RJ, Wareham NJ, Mustelin L, Rantanen T, Surakka I, Imboden M, Wichmann HE, Grkovic I, Jankovic S, Zgaga L, Hartikainen AL, Peltonen L, Gyllensten U, Johansson A, Zaboli G, Campbell H, Wild SH, Wilson JF, Glaser S, Homuth G, Volzke H, Mangino M, Soranzo N, Spector TD, Polasek O, Rudan I, Wright AF, Heliovaara M, Ripatti S, Pouta A, Naluai AT, Olin AC, Toren K, Cooper MN, James AL, Palmer LJ, Hingorani AD, Wannamethee SG,

Whincup PH, Smith GD, Ebrahim S, McKeever TM, Pavord ID, MacLeod AK, Morris AD, Porteous DJ, Cooper C, Dennison E, Shaheen S, Karrasch S, Schnabel E, Schulz H, Grallert H, Bouatia-Naji N, Delplanque J, Froguel P, Blakey JD, Britton JR, Morris RW, Holloway JW, Lawlor DA, Hui J, Nyberg F, Jarvelin MR, Jackson C, Kahonen M, Kaprio J, Probst-Hensch NM, Koch B, Hayward C, Evans DM, Elliott P, Strachan DP, Hall IP, Tobin MD. Genome-wide association study identifies five loci associated with lung function. *Nat Genet* 2010;42:36-44.

12. Hancock DB, Eijgelsheim M, Wilk JB, Gharib SA, Loehr LR, Marciante KD, Franceschini N, van Durme YM, Chen TH, Barr RG, Schabath MB, Couper DJ, Brusselle GG, Psaty BM, van Duijn CM, Rotter JI, Uitterlinden AG, Hofman A, Punjabi NM, Rivadeneira F, Morrison AC, Enright PL, North KE, Heckbert SR, Lumley T, Stricker BH, O'Connor GT, London SJ. Meta-analyses of genome-wide association studies identify multiple loci associated with pulmonary function. *Nat Genet* 2010;42:45-52.

13. Imboden M, Bouzigon E, Curjuric I, Ramasamy A, Kumar A, Hancock DB, Wilk JB, Vonk JM, Thun GA, Siroux V, Nadif R, Monier F, Gonzalez JR, Wjst M, Heinrich J, Loehr LR, Franceschini N, North KE, Altmuller J, Koppelman GH, Guerra S, Kronenberg F, Lathrop M, Moffatt MF, O'Connor GT, Strachan DP, Postma DS, London SJ, Schindler C, Kogevinas M, Kauffmann F, Jarvis DL, Demenais F, Probst-Hensch NM. Genome-wide association study of lung function decline in adults with and without asthma. *J Allergy Clin Immunol* 2012;129:1218-1228.

14. Yao TC, Du G, Han L, Sun Y, Hu D, Yang JJ, Mathias R, Roth LA, Rafaels N, Thompson EE, Loisel DA, Anderson R, Eng C, Arruabarrena Orbegozo M, Young M, Klocksieben JM, Anderson E, Shanovich K, Lester LA, Williams LK, Barnes KC, Burchard EG, Nicolae DL, Abney M, Ober C. Genome-wide association study of lung function phenotypes in a founder population. *J Allergy Clin Immunol* 2013;133:248-255.

15. Soler Artigas M, Loth DW, Wain LV, Gharib SA, Obeidat M, Tang W, Zhai G, Zhao JH, Smith AV, Huffman JE, Albrecht E, Jackson CM, Evans DM, Cadby G, Fornage M, Manichaikul A, Lopez LM, Johnson T, Aldrich MC, Aspelund T, Barroso I, Campbell H, Cassano PA, Couper DJ, Eiriksdottir G, Franceschini N, Garcia M, Gieger C, Gislason GK, Grkovic I, Hammond CJ, Hancock DB, Harris TB, Ramasamy A, Heckbert SR, Heliovaara M, Homuth G, Hysi PG, James AL, Jankovic S, Joubert BR, Karrasch S, Klopp N, Koch B, Kritchevsky SB, Launer LJ, Liu Y, Loehr LR, Lohman K, Loos RJ, Lumley T, Al Balushi KA, Ang WQ, Barr RG, Beilby J, Blakey JD, Boban M, Boraska V, Brisman J, Britton JR, Brusselle GG, Cooper C, Curjuric I, Dahgam S, Deary IJ, Ebrahim S, Eijgelsheim M, Francks C, Gaysina D, Granell R, Gu X, Hankinson JL, Hardy R, Harris SE, Henderson J, Henry A, Hingorani AD, Hofman A, Holt PG, Hui J, Hunter ML, Imboden M, Jameson KA, Kerr SM, Kolcic I, Kronenberg F, Liu JZ, Marchini J, McKeever T, Morris AD, Olin AC, Porteous DJ, Postma DS, Rich SS, Ring SM, Rivadeneira F, Rochat T, Sayer AA, Sayers I, Sly PD, Smith GD, Sood A, Starr JM, Uitterlinden AG, Vonk JM, Wannamethee SG, Whincup PH, Wijmenga C,

AJRCMB Articles in Press. Published on 09-May-2014 as 10.1165/rcmb.2013-0471OC

Williams OD, Wong A, Mangino M, Marciante KD, McArdle WL, Meibohm B, Morrison AC, North KE, Omenaas E, Palmer LJ, Pietilainen KH, Pin I, Pola Sbreve Ek O, Pouta A, Psaty BM, Hartikainen AL, Rantanen T, Ripatti S, Rotter JI, Rudan I, Rudnicka AR, Schulz H, Shin SY, Spector TD, Surakka I, Vitart V, Volzke H, Wareham NJ, Warrington NM, Wichmann HE, Wild SH, Wilk JB, Wjst M, Wright AF, Zgaga L, Zemunik T, Pennell CE, Nyberg F, Kuh D, Holloway JW, Boezen HM, Lawlor DA, Morris RW, Probst-Hensch N, Kaprio J, Wilson JF, Hayward C, Kahonen M, Heinrich J, Musk AW, Jarvis DL, Glaser S, Jarvelin MR, Ch Stricker BH, Elliott P, O'Connor GT, Strachan DP, London SJ, Hall IP, Gudnason V, Tobin MD. Genome-wide association and large-scale follow up identifies 16 new loci influencing lung function. *Nat Genet* 2011;43:1082-1090.

16. Hancock DB, Artigas MS, Gharib SA, Henry A, Manichaikul A, Ramasamy A, Loth DW, Imboden M, Koch B, McArdle WL, Smith AV, Smolonska J, Sood A, Tang W, Wilk JB, Zhai G, Zhao JH, Aschard H, Burkart KM, Curjuric I, Eijgelsheim M, Elliott P, Gu X, Harris TB, Janson C, Homuth G, Hysi PG, Liu JZ, Loehr LR, Lohman K, Loos RJ, Manning AK, Marciante KD, Obeidat M, Postma DS, Aldrich MC, Brusselle GG, Chen TH, Eiriksdottir G, Franceschini N, Heinrich J, Rotter JI, Wijmenga C, Williams OD, Bentley AR, Hofman A, Laurie CC, Lumley T, Morrison AC, Joubert BR, Rivadeneira F, Couper DJ, Kritchevsky SB, Liu Y, Wjst M, Wain LV, Vonk JM, Uitterlinden AG, Rochat T, Rich SS, Psaty BM, O'Connor GT, North KE, Mirel DB, Meibohm B, Launer LJ, Khaw KT, Hartikainen AL, Hammond CJ, Glaser S, Marchini J, Kraft P, Wareham NJ, Volzke H, Stricker BH, Spector TD, Probst-Hensch NM, Jarvis D, Jarvelin MR, Heckbert SR, Gudnason V, Boezen HM, Barr RG, Cassano PA, Strachan DP, Fornage M, Hall IP, Dupuis J, Tobin MD, London SJ. Genome-wide joint meta-analysis of snp and snp-by-smoking interaction identifies novel loci for pulmonary function. *PLoS Genet* 2012;8:e1003098.

17. Eichler EE, Flint J, Gibson G, Kong A, Leal SM, Moore JH, Nadeau JH. Missing heritability and strategies for finding the underlying causes of complex disease. *Nature reviews Genetics* 2010;11:446-450.

18. Zuk O, Hechter E, Sunyaev SR, Lander ES. The mystery of missing heritability: Genetic interactions create phantom heritability. *Proc Natl Acad Sci U S A* 2012;109:1193-1198.

19. Reinhard C, Eder G, Fuchs H, Ziesenis A, Heyder J, Schulz H. Inbred strain variation in lung function. *Mamm Genome* 2002;13:429-437.

20. Reinhard C, Meyer B, Fuchs H, Stoeger T, Eder G, Ruschendorf F, Heyder J, Nurnberg P, de Angelis MH, Schulz H. Genomewide linkage analysis identifies novel genetic loci for lung function in mice. *Am J Respir Crit Care Med* 2005;171:880-888.

21. Ganguly K, Stoeger T, Wesselkamper SC, Reinhard C, Sartor MA, Medvedovic M, Tomlinson CR, Bolle I, Mason JM, Leikauf GD, Schulz H. Candidate genes controlling pulmonary function in mice: Transcript profiling and predicted protein structure. *Physiol Genomics* 2007;31:410-421.

22. Ganguly K, Depner M, Fattman C, Bein K, Oury TD, Wesselkamper SC, Borchers MT, Schreiber M, Gao F, von Mutius E, Kabesch M, Leikauf GD, Schulz H. Superoxide dismutase 3, extracellular (SOD3) variants and lung function. *Physiol Genomics* 2009;37:260-267.

23. Lindsey JY, Ganguly K, Brass DM, Li Z, Potts EN, Degan S, Chen H, Brockway B, Abraham SN, Berndt A, Stripp BR, Foster WM, Leikauf GD, Schulz H, Hollingsworth JW. c-Kit is essential for alveolar maintenance and protection from emphysema-like disease in mice. *Am J Respir Crit Care Med* 2011;183:1644-1652.

24. Dahl M, Bowler RP, Juul K, Crapo JD, Levy S, Nordestgaard BG. Superoxide dismutase 3 polymorphism associated with reduced lung function in two large populations. *Am J Respir Crit Care Med* 2008;178:906-912.

25. Siedlinski M, van Diemen CC, Postma DS, Vonk JM, Boezen HM. Superoxide dismutases, lung function and bronchial responsiveness in a general population. *Eur Respir J* 2009;33:986-992.

26. Sorheim IC, DeMeo DL, Washko G, Litonjua A, Sparrow D, Bowler R, Bakke P, Pillai SG, Coxson HO, Lomas DA, Silverman EK, Hersh CP. Polymorphisms in the superoxide dismutase-3 gene are associated with emphysema in COPD. *COPD* 2010;7:262-268.

27. Pardo A, Gibson K, Cisneros J, Richards TJ, Yang Y, Becerril C, Yousem S, Herrera I, Ruiz V, Selman M, Kaminski N. Up-regulation and profibrotic role of osteopontin in human idiopathic pulmonary fibrosis. *PLoS Med* 2005;2:e251.

28. Schneider DJ, Lindsay JC, Zhou Y, Molina JG, Blackburn MR. Adenosine and osteopontin contribute to the development of chronic obstructive pulmonary disease. *FASEB J* 2010;24:70-80.

29. Ashkar S, Weber GF, Panoutsakopoulou V, Sanchirico ME, Jansson M, Zawaideh S, Rittling SR, Denhardt DT, Glimcher MJ, Cantor H. Eta-1 (osteopontin): An early component of type-1 (cell-mediated) immunity. *Science* 2000;287:860-864.

30. Chabas D, Baranzini SE, Mitchell D, Bernard CC, Rittling SR, Denhardt DT, Sobel RA, Lock C, Karpuj M, Pedotti R, Heller R, Oksenberg JR, Steinman L. The influence of the proinflammatory cytokine, osteopontin, on autoimmune demyelinating disease. *Science* 2001;294:1731-1735.

31. Liaw L, Birk DE, Ballas CB, Whitsitt JS, Davidson JM, Hogan BL. Altered wound healing in mice lacking a functional osteopontin gene (spp1). *J Clin Invest* 1998;101:1468-1478.

32. Trueblood NA, Xie Z, Communal C, Sam F, Ngoy S, Liaw L, Jenkins AW, Wang J, Sawyer DB, Bing OH, Apstein CS, Colucci WS, Singh K. Exaggerated left ventricular dilation and reduced collagen deposition after myocardial infarction in mice lacking osteopontin. *Circ Res* 2001;88:1080-1087.

AJRCMB Articles in Press. Published on 09-May-2014 as 10.1165/rcmb.2013-0471OC

33. Shen Q, Christakos S. Vitamin D receptor, Runx2, and the Notch signaling pathway cooperate in the transcriptional regulation of osteopontin. *J Biol Chem* 2005;280:40589-40598.

34. Sowa AK, Kaiser FJ, Eckhold J, Kessler T, Aherrahrou R, Wrobel S, Kaczmarek PM, Doehring L, Schunkert H, Erdmann J, Aherrahrou Z. Functional interaction of osteogenic transcription factors Runx2 and Vdr in transcriptional regulation of Opn during soft tissue calcification. *Am J Pathol* 2013;183:60-68.

35. Wikenheiser KA, Vorbroker DK, Rice WR, Clark JC, Bachurski CJ, Oie HK, Whitsett JA. Production of immortalized distal respiratory epithelial cell lines from surfactant protein c/simian virus 40 large tumor antigen transgenic mice. *Proc Natl Acad Sci U S A* 1993;90:11029-11033.

36. Nguyen NM, Bai Y, Mochitate K, Senior RM. Laminin alpha-chain expression and basement membrane formation by MLE-15 respiratory epithelial cells. *Am J Physiol Lung Cell Mol Physiol* 2002;282:L1004-L1011.

37. Schulz H, Johner C, Eder G, Ziesenis A, Reitmeier P, Heyder J, Balling R. Respiratory mechanics in mice: Strain and sex specific differences. *Acta Physiol Scand* 2002;174:367-375.

38. Cartharius K, Frech K, Grote K, Klocke B, Haltmeier M, Klingenhoff A, Frisch M, Bayerlein M, Werner T. MatInspector and beyond: promoter analysis based on transcription factor binding sites. *Bioinformatics* 2005;21: 2933-2942.

39. Huang DW, Sherman BT, Lempicki RA. Systematic and integrative analysis of large gene lists using DAVID Bioinformatics Resources. *Nature Protoc* 2009;4:44-57.

40. Huang DW, Sherman BT, Lempicki RA. Bioinformatics enrichment tools: paths toward the comprehensive functional analysis of large gene lists. *Nucleic Acids Res* 2009;37:1-13.

41. Friedmacher F, Doi T, Gosemann JH, Fujiwara N, Kutasy B, Puri P. Upregulation of fibroblast growth factor receptor 2 and 3 in the late stages of fetal lung development in the nitrofen rat model. *Pediatr Surg Int* 2012;28:195-199.

42. Shimoda LA, Semenza GL. HIF and the lung: Role of hypoxia-inducible factors in pulmonary development and disease. *Am J Respir Crit Care Med* 2011;183:152-156.

43. Pemberton AD, Rose-Zerilli MJ, Holloway JW, Gray RD, Holgate ST. A single-nucleotide polymorphism in intelectin 1 is associated with increased asthma risk. *J Allergy Clin Immunol* 2008;122:1033-1034.

44. Gu N, Kang G, Jin C, Xu Y, Zhang Z, Erle DJ, Zhen G. Intelectin is required for IL-13-induced monocyte chemotactic protein-1 and -3 expression in lung epithelial cells and promotes allergic airway inflammation. *Am J Physiol Lung Cell Mol Physiol* 2010;298:L290-L296.

45. Yamada N, Yamaya M, Okinaga S, Nakayama K, Sekizawa K, Shibahara S, Sasaki H. Microsatellite polymorphism in the heme oxygenase-1 gene promoter is associated with susceptibility to emphysema. *Am J Hum Genet* 2000;66:187-195.

46. Raval CM, Lee PJ. Heme oxygenase-1 in lung disease. *Curr Drug Targets* 2010;11:1532-1540.

47. Nie J, Pei D. Rapid inactivation of alpha-1-proteinase inhibitor by neutrophil specific leukolysin/membrane-type matrix metalloproteinase 6. *Exp Cell Res* 2004;296:145-150.

48. Sozo F, Hooper SB, Wallace MJ. Thrombospondin-1 expression and localization in the developing ovine lung. *J Physiol* 2007;584:625-635.

49. Zhao Y, Xiong Z, Lechner EJ, Klenotic PA, Hamburg BJ, Hulver M, Khare A, Oriss T, Mangalmurti N, Chan Y, Zhang Y, Ross MA, Stolz DB, Rosengart MR, Pilewski J, Ray P, Ray A, Silverstein RL, Lee JS. Thrombospondin-1 triggers macrophage il-10 production and promotes resolution of experimental lung injury. *Mucosal Immunol* 2014;7:440-448..

50. Wurfel MM, Gordon AC, Holden TD, Radella F, Strout J, Kajikawa O, Ruzinski JT, Rona G, Black RA, Stratton S, Jarvik GP, Hajjar AM, Nickerson DA, Rieder M, Sevransky J, Maloney JP, Moss M, Martin G, Shanholtz C, Garcia JG, Gao L, Brower R, Barnes KC, Walley KR, Russell JA, Martin TR. Toll-like receptor 1 polymorphisms affect innate immune responses and outcomes in sepsis. *Am J Respir Crit Care Med* 2008;178:710-720.

51. Thompson CM, Holden TD, Rona G, Laxmanan B, Black RA, O'Keefe GE, Wurfel MM. Toll-like receptor 1 polymorphisms and associated outcomes in sepsis after traumatic injury: A candidate gene association study. *Ann Surg* 2014;259:179-185.

52. Blohmke CJ, Park J, Hirschfeld AF, Victor RE, Schneiderman J, Stefanowicz D, Chilvers MA, Durie PR, Corey M, Zielenski J, Dorfman R, Sandford AJ, Daley D, Turvey SE. TLR5 as an anti-inflammatory target and modifier gene in cystic fibrosis. *J Immunol* 2010;185:7731-7738.

53. Lee CG, Dela Cruz CS, Ma B, Ahangari F, Zhou Y, Halaban R, Sznol M, Elias JA. Chitinase-like proteins in lung injury, repair, and metastasis. *Proc Am Thorac Soc* 2012;9:57-61.

54. Ortega H, Prazma C, Suruki RY, Li H, Anderson WH. Association of CHI3L1 in African-Americans with prior history of asthma exacerbations and stress. *J Asthma* 2013;50:7-13.

55. Kim YS, Choi SJ, Choi JP, Jeon SG, Oh S, Lee BJ, Gho YS, Lee CG, Zhu Z, Elias JA, Kim YK. IL-12-STAT4-IFN-gamma axis is a key downstream pathway in the development of IL-13-mediated asthma phenotypes in a Th2 type asthma model. *Exp Mol Med* 2010;42:533-546.

AJRCMB Articles in Press. Published on 09-May-2014 as 10.1165/rcmb.2013-0471OC

56. Yoshida M, Watson RM, Rerecich T, O'Byrne PM. Different profiles of T-cell IFN-gamma and IL-12 in allergen-induced early and dual responders with asthma. *J Allergy Clin Immunol* 2005;115:1004-1009.

57. Shu W, Lu MM, Zhang Y, Tucker PW, Zhou D, Morrisey EE. Foxp2 and Foxp1 cooperatively regulate lung and esophagus development. *Development* 2007;134:1991-2000.

58. Collison A, Hatchwell L, Verrills N, Wark PA, de Siqueira AP, Tooze M, Carpenter H, Don AS, Morris JC, Zimmermann N, Bartlett NW, Rothenberg ME, Johnston SL, Foster PS, Mattes J. The E3 ubiquitin ligase midline 1 promotes allergen and rhinovirus-induced asthma by inhibiting protein phosphatase 2A activity. *Nat Med* 2013;19:232-237.

59. Wang Y, Wimmer U, Lichtlen P, Inderbitzin D, Stieger B, Meier PJ, Hunziker L, Stallmach T, Forrer R, Rulicke T, Georgiev O, Schaffner W. Metal-responsive transcription factor-1 (MTF-1) is essential for embryonic liver development and heavy metal detoxification in the adult liver. *FASEB J* 2004;18:1071-1079.

60. Chang DR, Martinez Alanis D, Miller RK, Ji H, Akiyama H, McCrea PD, Chen J. Lung epithelial branching program antagonizes alveolar differentiation. *Proc Natl Acad Sci U S A* 2013;110:18042-18051.

61. Hersh CP, Silverman EK, Gascon J, Bhattacharya S, Klanderman BJ, Litonjua AA, Lefebvre V, Sparrow D, Reilly JJ, Anderson WH, Lomas DA, Mariani TJ. SOX5 is a candidate gene for chronic obstructive pulmonary disease susceptibility and is necessary for lung development. *Am J Respir Crit Care Med* 2011;183:1482-1489.

62. Gronostajski RM. Roles of the NFI/CTF gene family in transcription and development. *Gene* 2000;249:31-45.

63. Teves ME, Zhang Z, Costanzo RM, Henderson SC, Corwin FD, Zweit J, Sundaresan G, Subler M, Salloum FN, Rubin BK, Strauss JF, 3rd. Sperm-associated antigen-17 gene is essential for motile cilia function and neonatal survival. *Am J Respir Cell Mol Biol* 2013;48:765-772.

64. Cruciat CM, Dolde C, de Groot RE, Ohkawara B, Reinhard C, Korswagen HC, Niehrs C. RNA helicase DDX3 is a regulatory subunit of casein kinase 1 in Wnt-beta-catenin signaling. *Science* 2013;339:1436-1441.

65. Klinger S, Turgeon B, Levesque K, Wood GA, Aagaard-Tillery KM, Meloche S. Loss of ERK3 function in mice leads to intrauterine growth restriction, pulmonary immaturity, and neonatal lethality. *Proc Natl Acad Sci U S A* 2009;106:16710-16715.

66. Kramer EL, Hardie WD, Mushaben EM, Acciani TH, Pastura PA, Korfhagen TR, Hershey GK, Whitsett JA, Le Cras TD. Rapamycin decreases airway remodeling and hyperreactivity in a transgenic model of noninflammatory lung disease. *J Appl Physiol (1985)* 2011;111:1760-1767.

67. Mozaffarian A, Brewer AW, Trueblood ES, Luzina IG, Todd NW, Atamas SP, Arnett HA. Mechanisms of oncostatin M-induced pulmonary inflammation and fibrosis. *J Immunol* 2008;181:7243-7253.

68. Nogueira-Silva C, Piairo P, Carvalho-Dias E, Veiga C, Moura RS, Correia-Pinto J. The role of glycoprotein 130 family of cytokines in fetal rat lung development. *PLoS One* 2013;8:e67607.

69. Kormann MS, Depner M, Hartl D, Klopp N, Illig T, Adamski J, Vogelberg C, Weiland SK, von Mutius E, Kabesch M. Toll-like receptor heterodimer variants protect from childhood asthma. *J Allergy Clin Immunol* 2008;122:86-92.

70. Kesimer M, Ehre C, Burns KA, Davis CW, Sheehan JK, Pickles RJ. Molecular organization of the mucins and glycocalyx underlying mucus transport over mucosal surfaces of the airways. *Mucosal Immunol* 2013;6:379-392.

71. Leikauf GD, Borchers MT, Prows DR, Simpson LG. Mucin apoprotein expression in COPD. *Chest* 2002;121:166S-182S.

72. Shi W, Chen H, Sun J, Chen C, Zhao J, Wang YL, Anderson KD, Warburton D. Overexpression of Smurf1 negatively regulates mouse embryonic lung branching morphogenesis by specifically reducing Smad1 and Smad5 proteins. *Am J Physiol Lung Cell Mol Physiol* 2004;286:L293-L300.

73. Xu B, Chen C, Chen H, Zheng SG, Bringas P, Jr., Xu M, Zhou X, Chen D, Umans L, Zwijsen A, Shi W. Smad1 and its target gene Wif1 coordinate BMP and Wnt signaling activities to regulate fetal lung development. *Development* 2011;138:925-935.

74. Taylor BK, Stoops TD, Everett AD. Protein phosphatase inhibitors arrest cell cycle and reduce branching morphogenesis in fetal rat lung cultures. *Am J Physiol Lung Cell Mol Physiol* 2000;278:L1062-L1070.

75. Kobayashi Y, Mercado N, Barnes PJ, Ito K. Defects of protein phosphatase 2A causes corticosteroid insensitivity in severe asthma. *PLoS One* 2011;6:e27627.

76. Kaarteenaho R, Merikallio H, Lehtonen S, Harju T, Soini Y. Divergent expression of claudin -1, -3, -4, -5 and -7 in developing human lung. *Respir Res* 2010;11:59.

77. Jang AS, Concel VJ, Bein K, Brant KA, Liu S, Pope-Varsalona H, Dopico RA, Jr., Di YP, Knoell DL, Barchowsky A, Leikauf GD. Endothelial dysfunction and claudin 5 regulation during acrolein-induced lung injury. *Am J Respir Cell Mol Biol* 2011;44:483-490.

AJRCMB Articles in Press. Published on 09-May-2014 as 10.1165/rcmb.2013-0471OC

78. Ohta H, Chiba S, Ebina M, Furuse M, Nukiwa T. Altered expression of tight junction molecules in alveolar septa in lung injury and fibrosis. *Am J Physiol Lung Cell Mol Physiol* 2012;302:L193-L205.

79. Tao T, Lan J, Presley JF, Sweezey NB, Kaplan F. Nucleocytoplasmic shuttling of lgl2 is developmentally regulated in fetal lung. *Am J Respir Cell Mol Biol* 2004;30:350-359.

80. Diez-Roux G, Banfi S, Sultan M, Geffers L, Anand S, Rozado D, Magen A, Canidio E, Pagani M, Peluso I, Lin-Marq N, Koch M, Bilio M, Cantiello I, Verde R, De Masi C, Bianchi SA, Cicchini J, Perroud E, Mehmeti S, Dagand E, Schrinner S, Nurnberger A, Schmidt K, Metz K, Zwingmann C, Brieske N, Springer C, Hernandez AM, Herzog S, Grabbe F, Sieverding C, Fischer B, Schrader K, Brockmeyer M, Dettmer S, Helbig C, Alunni V, Battaini MA, Mura C, Henrichsen CN, Garcia-Lopez R, Echevarria D, Puelles E, Garcia-Calero E, Kruse S, Uhr M, Kauck C, Feng G, Milyaev N, Ong CK, Kumar L, Lam M, Semple CA, Gyenesei A, Mundlos S, Radelof U, Lehrach H, Sarmientos P, Reymond A, Davidson DR, Dolle P, Antonarakis SE, Yaspo ML, Martinez S, Baldock RA, Eichele G, Ballabio A. A high-resolution anatomical atlas of the transcriptome in the mouse embryo. *PLoS Biol* 2011;9:e1000582.

81. Morrisey EE, Hogan BL. Preparing for the first breath: genetic and cellular mechanisms in lung development. *Dev Cell* 2010;18:8-23.

82. Lavoie PM, Pham C, Jang KL. Heritability of bronchopulmonary dysplasia, defined according to the consensus statement of the national institutes of health. *Pediatrics* 2008;122:479-485.

83. Gough A, Linden M, Spence D, Patterson CC, Halliday HL, McGarvey LP. Impaired lung function and health status in adult survivors of bronchopulmonary dysplasia. *Eur Respir J* 2013. [Epub ahead of print]

84. Massaro D, Massaro GD. Critical period for alveologenesis and early determinants of adult pulmonary disease. *Am J Physiol Lung Cell Mol Physiol* 2004;287:L715-L717.

85. Martinez FD. The origins of asthma and chronic obstructive pulmonary disease in early life. *Proc Am Thorac Soc* 2009;6:272-277.

86. Svanes C, Sunyer J, Plana E, Dharmage S, Heinrich J, Jarvis D, de Marco R, Norback D, Raherison C, Villani S, Wjst M, Svanes K, Anto JM. Early life origins of chronic obstructive pulmonary disease. *Thorax* 2010;65:14-20.

87. Stocks J, Sonnappa S. Early life influences on the development of chronic obstructive pulmonary disease. *Ther Adv Respir Dis* 2013;7:161-173.

88. Shi W, Bellusci S, Warburton D. Lung development and adult lung diseases. *Chest* 2007;132:651-656.

89. Warburton D, Schwarz M, Tefft D, Flores-Delgado G, Anderson KD, Cardoso WV. The molecular basis of lung morphogenesis. *Mech Dev* 2000;92:55-81.

90. Warburton D, Bellusci S, Del Moral PM, Kaartinen V, Lee M, Tefft D, Shi W. Growth factor signaling in lung morphogenetic centers: Automaticity, stereotypy and symmetry. *Respir Res* 2003;4:5.

91. Warburton D, Bellusci S, De Langhe S, Del Moral PM, Fleury V, Mailleux A, Tefft D, Unbekandt M, Wang K, Shi W. Molecular mechanisms of early lung specification and branching morphogenesis. *Pediatr Res* 2005;57:26R-37R.

92. Shi W, Xu J, Warburton D. Development, repair and fibrosis: what is common and why it matters. *Respirology* 2009;14:656-665.

93. Mitzner W. Use of mean airspace chord length to assess emphysema. *J Appl Physiol* 2008;105:1980-1981

94. Giacopelli F, Marciano R, Pistorio A, Catarsi P, Canini S, Karsenty G, Ravazzolo R. Polymorphisms in the osteopontin promoter affect its transcriptional activity. *Physiol Genomics* 2004;20:87-96.

95. Schultz J, Lorenz P, Ibrahim SM, Kundt G, Gross G, Kunz M. The functional -443T/C osteopontin promoter polymorphism influences osteopontin gene expression in melanoma cells via binding of c-Myb transcription factor. *Mol Carcinog* 2009;48:14-23.\

96. D'Alfonso S1, Barizzone N, Giordano M, Chiocchetti A, Magnani C, Castelli L, Indelicato M, Giacopelli F, Marchini M, Scorza R, Danieli MG, Cappelli M, Migliaresi S, Bigliardo B, Sabbadini MG, Baldissera E, Galeazzi M, Sebastiani GD, Minisola G, Ravazzolo R, Dianzani U, Momigliano-Richiardi P. Two single-nucleotide polymorphisms in the 5' and 3' ends of the osteopontin gene contribute to susceptibility to systemic lupus erythematosus. *Arthritis Rheum* 2005;52:539–547

97. Kariuki SN, Moore JG, Kirou KA, Crow MK, Utset TO, Niewold TB. Age- and gender-specific modulation of serum osteopontin and interferon-alpha by osteopontin genotype in systemic lupus erythematosus. *Genes Immun* 2009;10:487-494.

98. Barizzone N, Marchini M, Cappiello F, Chiocchetti A, Orilieri E, Ferrante D, Corrado L, Mellone S, Scorza R, Dianzani U, D'Alfonso S. Association of osteopontin regulatory polymorphisms with systemic sclerosis. *Hum Immunol* 2011;72:930-934.

99. Glas J, Seiderer J, Bayrle C, Wetzke M, Fries C, Tillack C, Olszak T, Beigel F, Steib C, Friedrich M, Diegelmann J, Czamara D, Brand S. The role of osteopontin (OPN/SPP1) haplotypes in the susceptibility to Crohn's disease. *PLoS One* 2011;6:e29309.

100. Gazal S, Sacre K, Allanore Y, Teruel M, Goodall AH; (The CARDIOGENICS consortium), Tohma S, Alfredsson L, Okada Y, Xie G, Constantin A, Balsa A, Kawasaki A, Nicaise P, Amos C, Rodriguez-

AJRCMB Articles in Press. Published on 09-May-2014 as 10.1165/rcmb.2013-0471OC

Rodriguez L, Chioccia G, Boileau C, Zhang J, Vittecoq O, Barnetche T, Gonzalez Gay MA, Furukawa H, Cantagrel A, Le Loët X, Sumida T, Hurtado-Nedelec M, Richez C, Chollet-Martin S, Schaeverbeke T, Combe B, Khoryati L, Coustet B, El-Benna J, Siminovitch K, Plenge R, Padyukov L, Martin J, Tsuchiya N, Dieudé P. Identification of secreted phosphoprotein 1 gene as a new rheumatoid arthritis susceptibility gene. *Ann Rheum Dis* 2014 [Epub ahead of print].

101. Zhang Z, Deepak V, Meng L, Wang L, Li Y, Jiang Q, Zeng X, Liu W. Analysis of HDAC1-mediated regulation of Runx2-induced osteopontin gene expression in C3h10t1/2 cells. *Biotechnol Lett* 2012;34:197-203.

102. Hollingsworth JW, Maruoka S, Boon K, Garantziotis S, Li Z, Tomfohr J, Bailey N, Potts EN, Whitehead G, Brass DM, Schwartz DA. In utero supplementation with methyl donors enhances allergic airway disease in mice. *J Clin Invest* 2008;118:3462-3469.

103. Haley KJ, Lasky-Su J, Manoli SE, Smith LA, Shahsafaei A, Weiss ST, Tantisira K. RUNX transcription factors: association with pediatric asthma and modulated by maternal smoking. *Am J Physiol Lung Cell Mol Physiol* 2011;301:L693-L701.

104. Srisuma S, Bhattacharya S, Simon DM, Solleti SK, Tyagi S, Starcher B, Mariani TJ. Fibroblast growth factor receptors control epithelial-mesenchymal interactions necessary for alveolar elastogenesis. *Am J Respir Crit Care Med* 2010;181:838-850.

105. Powell-Braxton L, Hollingshead P, Warburton C, Dowd M, Pitts-Meek S, Dalton D, Gillett N, Stewart TA. IGF-I is required for normal embryonic growth in mice. *Genes Dev* 1993;7:2609-2617

106. Briscoe J, Therond PP. The mechanisms of hedgehog signalling and its roles in development and disease. *Nat Rev Mol Cell Biol* 2013;14:416-429.

107. Chuang PT, Kawcak T, McMahon AP. Feedback control of mammalian Hedgehog signaling by the Hedgehog-binding protein, Hip1, modulates Fgf signaling during branching morphogenesis of the lung. *Genes Dev* 2003;17:342-347.

108. Kerkhof M, Boezen HM, Granell R, Wijga AH, Brunekreef B, Smit HA, de Jongste JC, Thijs C, Mommers M, Penders J, Henderson J, Koppelman GH, Postma DS. Transient early wheeze and lung function in early childhood associated with chronic obstructive pulmonary disease genes. *J Allergy Clin Immunol* 2014;133:68-76.

109. Pillai SG, Ge D, Zhu G, Kong X, Shianna KV, Need AC, Feng S, Hersh CP, Bakke P, Gulsvik A, Ruppert A, Lodrup Carlsen KC, Roses A, Anderson W, Rennard SI, Lomas DA, Silverman EK, Goldstein DB. A genome-wide association study in chronic obstructive pulmonary disease (COPD): identification of two major susceptibility loci. *PLoS Genet* 2009;5:e1000421.

110. Zhou X, Baron RM, Hardin M, Cho MH, Zielinski J, Hawrylkiewicz I, Sliwinski P, Hersh CP, Mancini JD, Lu K, Thibault D, Donahue AL, Klanderman BJ, Rosner B, Raby BA, Lu Q, Geldart AM, Layne MD, Perrella MA, Weiss ST, Choi AM, Silverman EK. Identification of a chronic obstructive pulmonary disease genetic determinant that regulates HHIP. *Hum Mol Genet* 2012;21:1325-1335.

111. Lamontagne M, Couture C, Postma DS, Timens W, Sin DD, Pare PD, Hogg JC, Nickle D, Laviolette M, Bosse Y. Refining susceptibility loci of chronic obstructive pulmonary disease with lung eqtls. *PLoS One* 2013;8:e70220.

112. Li C, Xiao J, Hormi K, Borok Z, Minoo P. Wnt5a participates in distal lung morphogenesis. *Dev Biol* 2002;248:68-81.

113. Li C, Hu L, Xiao J, Chen H, Li JT, Bellusci S, Delanghe S, Minoo P. Wnt5a regulates Shh and Fgf10 signaling during lung development. *Dev Biol* 2005;287:86-97.

114. Collins BJ, Kleeberger W, Ball DW. Notch in lung development and lung cancer. *Semin Cancer Biol* 2004;14, 357-364.

115. Rock JR, Gao X, Xue Y, Randell SH, Kong YY, Hogan BL. Notch-dependent differentiation of adult airway basal stem cells. *Cell Stem Cell* 2011;8:639–64

116. Guseh JS, Bores SA, Stanger BZ, Zhou Q, Anderson WJ, Melton DA, Rajagopal J. Notch signaling promotes airway mucous metaplasia and inhibits alveolar development. *Development* 2009;136:1751-1759.

117. Tsao PN, Vasconcelos M, Izvolsky KI, Qian J, Lu J, Cardoso WV. Notch signaling controls the balance of ciliated and secretory cell fates in developing airways. *Development* 2009;136:2297-2307.

AJRCMB Articles in Press. Published on 09-May-2014 as 10.1165/rcmb.2013-0471OC

Table 1. Lung function values of 27 inbred mouse strains (Gender = female, Total = 252 mice).

Strain	n	Age*	BW*	BW SE	TLC*	TLC SE	TLC/BW*	TLC/BW SE	sC_L*	sC_L SE	V_D*	V_D SE
AKR/J	8	16.0	30.6	1.2	1176	32	40.9	1.5	49.8	2.7	231	4
BALB/cJ	10	13.9	22.7	0.8	1277	17	60.2	2.5	63.9	3.0	233	2
BPL/1J	10	14.2	16.9	0.4	1046	16	66.5	1.7	72.4	3.2	230	2
BTBR *T*$^+$ *tf*/J	8	13.9	31.9	0.6	1409	26	46.5	1.6	58.2	1.7	251	3
BUB/BnJ	10	14.1	25.6	0.6	1097	38	45.1	1.2	58.0	3.2	225	2
C3HeB/FeJ	10	14.4	25.7	0.9	1480	33	61.6	2.3	72.9	4.0	232	3
C57BL/10J	10	14.3	20.7	0.4	1034	11	52.7	1.0	51.2	0.7	233	4
C57BLKS/J	10	14.3	21.7	0.6	1131	24	54.8	1.2	55.6	2.7	233	5
C57BR/cdJ	9	13.9	24.0	1.1	1116	28	49.1	2.2	54.4	3.0	221	4
C57L/J	9	15.8	22.7	0.3	1209	26	55.8	0.9	55.0	1.3	244	2
C58/J	10	14.7	19.8	0.5	1002	20	53.7	0.9	53.2	1.1	215	2
CBA/J	10	15.3	28.6	0.5	1177	17	43.4	0.9	59.8	3.4	242	1
DBA/1J	8	16.4	20.9	0.5	971	14	49.2	1.4	52.7	2.1	231	5
DBA/2J	8	15.4	24.2	0.8	1054	17	45.8	1.7	58.0	1.3	232	3
KK/HlJ	7	13.9	35.0	1.3	1304	29	39.6	1.5	47.0	1.9	246	2
LP/J	8	14.3	18.9	0.5	1074	29	59.6	1.7	61.6	2.9	241	4
MRL/MpJ	10	13.9	35.5	1.3	1519	42	45.0	1.1	56.3	3.7	251	3
NOD/ShiLtJ	8	15.1	21.9	0.6	1012	25	48.8	1.6	60.7	2.4	222	2
NON/ShiLtJ	8	14.3	31.3	0.9	1426	26	48.4	1.6	75.1	3.2	255	2
NZL/LtJ	9	14.4	36.3	1.9	1409	34	41.9	2.2	59.6	2.5	230	2
NZW/LacJ	8	14.3	27.4	0.8	1218	26	46.8	0.7	75.9	5.5	250	4
PL/J	10	14.1	20.5	0.7	956	13	49.7	1.2	49.0	1.2	210	3
PWD/PhJ	14	15.2	15.8	0.3	967	21	64.8	1.5	33.4	1.2	202	5
RIIIS/J	10	14.2	17.8	0.4	995	25	59.2	2.0	55.1	3.3	221	3
SJL/J	10	13.9	20.2	0.5	857	11	44.6	1.2	48.5	2.1	198	5
SM/J	10	15.4	14.1	0.3	881	25	62.6	1.6	47.1	2.3	222	7
WSB/EiJ	10	14.9	14.3	0.3	744	28	53.8	1.9	40.8	1.7	201	4

Abbreviations: **n** = number of mice phenotyped/strain; **Age** in weeks; **SE**= standard error; **BW** = body weight (g); **TLC** = total lung capacity (μl); **TLC/BW** = specific total lung capacity (μl/g); **sC_L** = specific static compliance of the lung = **C_L/TLC** in ml (μl/cm H_2O/ml TLC); **V_D** = dead space volume (μl). *Values are means.

Table 2. Increased Lung Transcripts in Secreted Phosphoprotein 1 Deficient Mice at Postnatal Day 14

Gene Symbol	Entrez Gene ID	Fold Change	p-value	Description
Molecular Function: GO:0004713 protein tyrosine kinase activity				Enrichment Score: 1.8
Dyrk1a	13548	2.24	0.002	dual-specificity tyrosine-(Y)-phosphorylation regulated kinase 1a
Ltk	17005	2.11	0.028	leukocyte tyrosine kinase
Fgfr3	14184	1.95	<0.001	fibroblast growth factor receptor 3
Map2k6	26399	1.82	0.005	mitogen-activated protein kinase kinase 6
Cdc7	12545	1.74	0.034	cell division cycle 7 (S. cerevisiae)
Tyk2	54721	1.64	<0.001	tyrosine kinase 2
Blk	12143	1.59	0.029	B lymphoid kinase
Epha5	13839	1.59	<0.001	Eph receptor A5
Ntrk2	18212	1.55	0.002	neurotrophic tyrosine kinase, receptor, type 2
Ephb3	13845	1.51	<0.001	Eph receptor B3
Biological Process: GO:0048514 blood vessel morphogenesis				Enrichment Score: 2.3
Hif1a	15251	2.14	0.005	hypoxia inducible factor 1, alpha subunit
Tbx20	57246	2.09	0.001	T-box 20
Wt1	22431	1.83	0.029	Wilms tumor 1 homolog
Hmox1	15368	1.69	0.001	heme oxygenase (decycling) 1
Foxm1	14235	1.67	0.027	forkhead box M1
Cav1	12389	1.58	0.018	caveolin 1, caveolae protein
Ovol2	107586	1.57	<0.001	ovo-like 2 (Drosophila)
Ntrk2	18212	1.55	0.002	neurotrophic tyrosine kinase, receptor, type 2
Dll4	54485	1.55	0.001	delta-like 4 (Drosophila)
Ccbe1	320924	1.51	0.014	collagen and calcium binding EGF domains 1
Tnni3	21954	1.50	0.045	troponin I, cardiac 3
Cellular Component: GO:0042995 cell projection				Enrichment Score: 2.8
Itln1	16429	4.32	0.018	intelectin 1 (galactofuranose binding)
Prph	19132	2.12	0.027	peripherin
Exph5	320051	2.03	0.005	exophilin 5
Myl7	17898	1.86	0.015	myosin, light polypeptide 7, regulatory
Dynlt1c	1E+08	1.80	<0.001	dynein light chain Tctex-type 1C
Ctnnd1	12388	1.79	0.020	catenin (cadherin associated protein), delta 1
Dpysl5	65254	1.71	0.001	dihydropyrimidinase-like 5
C2cd3	277939	1.67	0.050	C2 calcium-dependent domain containing 3
Cyth3	19159	1.67	0.006	cytohesin 3
Tesc	57816	1.64	0.024	tescalcin
KEGG Pathway: mmu05414: dilated cardiomyopathy				Enrichment Score: 1.9
Grik2	14806	2.68	0.001	glutamate receptor, ionotropic, kainate 2 (beta 2)
Myh6	17888	2.22	0.017	myosin, heavy polypeptide 6, cardiac muscle, alpha
Mybpc3	17868	2.09	0.004	myosin binding protein C, cardiac
Atp1a2	98660	1.88	0.006	ATPase, Na+/K+ transporting, alpha 2 polypeptide
Adrb1	11554	1.83	<0.001	adrenergic receptor, beta 1
Tnnc1	21924	1.80	0.035	troponin C, cardiac/slow skeletal
Adrb3	11556	1.72	<0.001	adrenergic receptor, beta 3
Actg1	11465	1.70	0.003	actin, gamma, cytoplasmic 1
Atp2a2	11938	1.66	0.004	ATPase, Ca++ transporting, cardiac muscle, slow twitch 2
Tnni3	21954	1.50	0.045	troponin I, cardiac 3

AJRCMB Articles in Press. Published on 09-May-2014 as 10.1165/rcmb.2013-0471OC

Table 3. Decreased Lung Transcripts in Secreted Phosphoprotein 1 Deficient Mice at Postnatal Day 14

Gene Symbol	Entrez Gene ID	Fold Change	p-value	Description
Molecular Function GO:0008233 peptidase activity				Enrichment Score: 2.4
Adamts4	240913	-5.8	0.005	a disintegrin-like and metallopeptidase (reprolysin type) with thrombospondin type 1 motif, 4
Adam28	13522	-2.5	0.007	a disintegrin and metallopeptidase domain 28
Agbl3	76223	-2.5	0.001	ATP/GTP binding protein-like 3
Mmel1	27390	-2.3	0.026	membrane metallo-endopeptidase-like 1
Adamdec1	58860	-2.2	0.044	ADAM-like, decysin 1
Qpct	70536	-1.8	0.042	glutaminyl-peptide cyclotransferase (glutaminyl cyclase)
Acr	11434	-1.7	0.037	acrosin prepropeptide
Ecel1	13599	-1.7	0.025	endothelin converting enzyme-like 1
Mmp25	240047	-1.6	0.004	matrix metallopeptidase 25
Usp36	72344	-1.5	0.003	ubiquitin specific peptidase 36
Biological Process GO:0009611 response to wounding				Enrichment Score: 1.5
Gp9	54368	-2.4	0.012	glycoprotein 9 (platelet)
Thbs1	21825	-2.1	0.010	thrombospondin 1
Tnfrsf1b	21938	-2.1	<0.001	tumor necrosis factor receptor superfamily, member 1b
Tlr1	21897	-2.0	0.033	toll-like receptor 1
P2ry12	70839	-1.9	0.003	purinergic receptor P2Y, G-protein coupled 12
Pf4	56744	-1.7	<0.001	platelet factor 4
Tlr5	53791	-1.6	0.048	toll-like receptor 5
Hps5	246694	-1.6	0.032	Hermansky-Pudlak syndrome 5 homolog (human)
Treml1	71326	-1.6	0.017	triggering receptor expressed on myeloid cells-like 1
Ccl19	24047	-1.5	0.029	chemokine (C-C motif) ligand 19
Cellular Component GO:0005615 extracellular space				Enrichment Score: 2.8
Afm	280662	-4.6	0.001	afamin
Enpp1	18605	-2.9	0.045	ectonucleotide pyrophosphatase/phosphodiesterase 1
Chi3l1	12654	-2.8	0.024	chitinase 3-like 1
Cilp	214425	-2.8	0.005	cartilage intermediate layer protein, nucleotide pyrophosphohydrolase
Spon2	100689	-2.7	0.016	spondin 2, extracellular matrix protein
Apoc2	11813	-2.7	0.025	apolipoprotein C-II
Adam28	13522	-2.5	0.007	a disintegrin and metallopeptidase domain 28
Gdf3	14562	-2.5	0.029	growth differentiation factor 3
Mmp8	17394	-2.4	0.034	matrix metallopeptidase 8
Grp	225642	-2.3	0.004	gastrin releasing peptide
KEGG Pathway mmu04060: cytokine-cytokine receptor interaction				Enrichment Score: 1.8
Ccr8	12776	-2.8	0.014	chemokine (C-C motif) receptor 8
Ccl7	20306	-2.4	0.047	chemokine (C-C motif) ligand 7
Cxcr2	12765	-2.3	0.010	chemokine (C-X-C motif) receptor 2
Tnfrsf13c	72049	-2.3	0.038	tumor necrosis factor receptor superfamily, member 13c
Tnfrsf9	21942	-2.1	0.039	tumor necrosis factor receptor superfamily, member 9
Ccl12	20293	-2.1	0.041	chemokine (C-C motif) ligand 12
Il12b	16160	-2.0	<0.001	interleukin 12b
Mpl	17480	-1.7	0.012	myeloproliferative leukemia virus oncogene
Pf4	56744	-1.7	>0.001	platelet factor 4
Inhbb	16324	-1.6	0.004	inhibin beta-B

Table 4. Increased Lung Transcripts in Secreted Phosphoprotein 1 Deficient Mice at Postnatal Day 28

Gene Symbol	Entrez Gene ID	Fold Change	p-value	Description
Molecular Function: GO:0008270 zinc ion binding				Enrichment Score: 9.2
Rag1	19373	11.07	0.013	recombination activating gene 1
Zfp14	243906	4.13	0.001	zinc finger protein 14
Trim59	66949	3.38	<0.001	tripartite motif-containing 59
Birc5	11799	2.82	0.016	baculoviral IAP repeat-containing 5
Snai2	20583	2.46	0.033	snail homolog 2 (Drosophila)
Foxp2	114142	2.06	0.024	forkhead box P2
Mid1	17318	1.97	0.034	midline 1
Naip6	17952	1.94	0.013	NLR family, apoptosis inhibitory protein 6
Rfwd2	26374	1.77	0.004	ring finger and WD repeat domain 2
Mtf1	17764	1.72	<0.001	metal response element binding transcription factor 1
Biological Process: GO:0045449 regulation of transcription				Enrichment Score: 14.3
Dnmt3a	13435	2.80	0.010	DNA methyltransferase 3A
Runx1	12394	2.67	0.008	runt related transcription factor 1
Sox9	20682	2.52	0.005	SRY-box containing gene 9
Ccna2	12428	2.39	0.044	cyclin A2
Sox5	20678	2.16	0.011	SRY-box containing gene 5
Myb	17863	2.15	0.009	myeloblastosis oncogene
Egr3	13655	2.02	0.042	early growth response 3
Maf	17132	1.98	0.028	avian musculoaponeurotic fibrosarcoma (v-maf) AS42 oncogene homolog
Nfia	18027	1.80	0.011	nuclear factor I/A
E2f2	242705	1.74	0.017	E2F transcription factor 2
Cellular Component: GO:0015630 microtubule cytoskeleton				Enrichment Score: 7.7
Tube1	71924	3.63	0.001	epsilon-tubulin 1
Aurka	20878	3.46	<0.001	aurora kinase A
Kifc1	1E+08	2.66	0.012	kinesin family member C1
Spag17	74362	2.36	0.005	sperm associated antigen 17
Tubd1	56427	2.22	0.001	tubulin, delta 1
Cep55	74107	2.01	<0.001	centrosomal protein 55
Haus8	76478	1.95	0.006	4HAUS augmin-like complex, subunit 8
Rpgrip1l	244585	1.83	0.021	Rpgrip1-like
Ttll7	70892	1.78	0.041	tubulin tyrosine ligase-like family, member 7
C2cd3	277939	1.72	0.016	C2 calcium-dependent domain containing 3
KEGG Pathway: mmu04110 cell cycle				Enrichment Score: 2.9
Cdk1	12534	2.92	0.036	cyclin-dependent kinase 1
Bub1	12235	2.89	0.001	budding uninhibited by benzimidazoles 1 homolog (S. cerevisiae)
Skp2	27401	2.70	0.002	S-phase kinase-associated protein 2 (p45)
Ccnb1	268697	2.47	0.004	cyclin B1
Ccna2	12428	2.39	0.044	cyclin A2
Chek2	50883	2.25	0.043	CHK2 checkpoint homolog (S. pombe)
Cdc20	107995	2.25	0.006	cell division cycle 20 homolog (S. cerevisiae)
Plk1	18817	2.10	0.008	polo-like kinase 1 (Drosophila)
Cdc25c	12532	2.09	0.038	cell division cycle 25 homolog C (S. pombe)
Anapc10	68999	1.81	0.011	anaphase promoting complex subunit 10

AJRCMB Articles in Press. Published on 09-May-2014 as 10.1165/rcmb.2013-0471OC

Table 5. Decreased Lung Transcripts in Secreted Phosphoprotein 1 Deficient Mice at Postnatal Day 28

Gene Symbol	Entrez Gene ID	Fold Change	p-value	Description
Molecular Function: GO:0004672 protein kinase activity				Enrichment Score: 2.4
Taok2	381921	-3.12	0.001	TAO kinase 2
Phkg1	18682	-3.03	0.003	phosphorylase kinase gamma 1
Tnk1	83813	-2.70	0.015	tyrosine kinase, non-receptor, 1
Csnk1e	27373	-2.64	0.002	casein kinase 1, epsilon
Mapk6	50772	-2.49	0.006	mitogen-activated protein kinase 6
Plk3	12795	-2.19	<0.001	polo-like kinase 3 (Drosophila)
Sgk2	27219	-2.16	0.025	serum/glucocorticoid regulated kinase 2
Irak2	108960	-2.15	0.025	interleukin-1 receptor-associated kinase 2
Mtor	56717	-2.14	0.005	mechanistic target of rapamycin (serine/threonine kinase)
Trib1	211770	-2.10	<0.001	tribbles homolog 1 (Drosophila)
Biological Process: GO:0007243 protein kinase cascade				Enrichment Score: 2.4
Gna13	14674	-3.06	<0.001	guanine nucleotide binding protein, alpha 13
Osm	18413	-2.82	0.005	oncostatin M
Tlr6	21899	-2.62	0.007	toll-like receptor 6
Muc20	224116	-2.18	0.048	mucin 20
Irak2	108960	-2.15	0.025	interleukin-1 receptor-associated kinase 2
Ghrl	58991	-2.00	0.005	ghrelin
Edn1	13614	-1.99	0.012	endothelin 1
Pxn	19303	-1.71	0.005	paxillin
Smad1	17125	-1.65	0.045	MAD homolog 1 (Drosophila)
Dapk3	13144	-1.62	0.045	death-associated protein kinase 3
Fgfr3	14184	-1.53	0.033	fibroblast growth factor receptor 3
Cellular Component: GO:0005911 cell-cell junction				Enrichment Score: 2.5
Myl2	17906	-8.71	0.027	myosin, light polypeptide 2, regulatory, cardiac, slow
Nrap	18175	-3.29	0.003	nebulin-related anchoring protein
Myh7	140781	-2.96	0.002	myosin, heavy polypeptide 7, cardiac muscle, beta
Ppp2ca	19052	-2.60	<0.001	protein phosphatase 2 (formerly 2A), catalytic subunit, alpha isoform
Csnk2a2	13000	-2.40	0.003	casein kinase 2, alpha prime polypeptide
Shroom3	27428	-2.27	0.016	shroom family member 3
Pcp4	18546	-2.10	0.006	Purkinje cell protein 4
Prkcz	18762	-2.07	0.005	protein kinase C, zeta
Ppp2r2b	72930	-2.05	0.039	protein phosphatase 2 (formerly 2A), regulatory subunit B (PR 52), beta isoform
Cldn23	71908	-1.88	0.023	claudin 23
KEGG Pathway: mmu04530: tight junction				Enrichment Score: 1.9
Exoc4	20336	-1.86	0.032	exocyst complex component 4
Gja4	14612	-1.81	0.001	gap junction protein, alpha 4
Pard6b	58220	-1.77	0.002	par-6 (partitioning defective 6) homolog beta (C. elegans)
Myh9	17886	-1.77	0.002	myosin, heavy polypeptide 9, non-muscle
Cldn4	12740	-1.70	0.039	claudin 4
Ahnak	66395	-1.70	0.020	AHNAK nucleoprotein (desmoyokin)
Cldn5	12741	-1.69	0.006	claudin 5
Llgl2	217325	-1.58	0.017	lethal giant larvae homolog 2 (Drosophila)
Cldn7	53624	-1.55	0.016	claudin 7
Cldn3	12739	-1.51	0.004	claudin 3

Figure Legends

Figure 1. Lung secreted phosphoprotein 1 (SPP1) transcript and protein decreased in JF1/Msf mice as compared to C3H/HeJ mice. A. During postnatal (P) lung development (P7-P70 days), lung SPP1 transcript decreased in JF1/Msf mice as compared to C3H/HeJ mice. Previously we determined that JF1/Msf mice have diminished lung function as compared to C3H/HeJ mice (20, 21). Reduced transcripts (~4-fold) were first noted at P14, which is the peak stage of alveologenesis. **B.** Lung SPP1 protein decreased 1.7-fold in P28 JF1/Msf mice as compared to P28 C3H/HeJ mice. Values are mean ± standard error (n = 5 mice/strain) and statistical significance (*p<0.05) was determined by analysis of variance (ANOVA) test and all pairwise comparisons procedure (Holm-Sidak method).

Figure 2. Genetic variant in secreted phosphoprotein 1 (*Spp1*) promoter alters nuclear protein binding capacity. Electrophoretic mobility shift assay of nuclear protein extract prepared from mouse lung epithelial cells (MLE-15) and 25-mer probes (-144bp to -168bp from the start site). Single nucleotide polymorphism rs264140167 (-158 nucleotides from the transcription start site) in the *Spp1* promoter region was used to generate 25-mer probes containing either the C3H/HeJ T allele or the JF1/Msf G allele in the middle of the biotinylated oligonucleotide. The C3H/HeJ T allele increased the DNA protein binding to form slow migrating complexes (arrow 1) and enhanced the intensity of a faster migrating complex (arrow 2) compared to the JF1/Msf G allele. The C3H/HeJ T allele forms an additional putative RUNX2 binding site not present in the JF1/Msf G allele.

Figure 3. Lung function measurements of secreted phosphoprotein 1 deficient (*Spp1*$^{(-/-)}$) mice compared to strain matched control (*Spp1*$^{(+/+)}$) mice. **(A)** *Spp1*$^{(-/-)}$ mice have 15% decreased total lung capacity (TLC) (*Spp1*$^{(-/-)}$ = 1034 ± 25 versus *Spp1*$^{(+/+)}$ = 1220 ± 22 µl. **(B)** *Spp1*$^{(-/-)}$ mice have 17% decreased specific TLC (TLC/body weight) (*Spp1*$^{(-/-)}$ = 48 ± 1 versus *Spp1*$^{(+/+)}$ = 58 ± 1 µl/g). (**C)** *Spp1*$^{(-/-)}$ mice have 14% increased specific compliance (sC_L) compared to *Spp1*$^{(+/+)}$ mice (*Spp1*$^{(-/-)}$ = 54 ±1 versus *Spp1*$^{(+/+)}$ = 47 ± 1 µl/cmH_2O / ml). Values are mean ± standard error (n= 8 mice/strain, age = 12-14 wk) and statistical significance (*p<0.001) was determined by analysis of variance (ANOVA) test and all pairwise comparisons procedure (Holm-Sidak method).

AJRCMB Articles in Press. Published on 09-May-2014 as 10.1165/rcmb.2013-0471OC

Figure 4. Comparison of alveolar air space size between secreted phosphoprotein 1 deficient (*Spp1*$^{(-/-)}$) and strain matched control (*Spp1*$^{(+/+)}$) mice at the age of 4 weeks when alveolarization is completed. Lung morphometric analysis revealed 14% increased mean chord length in *Spp1*$^{(-/-)}$ mice (L_m: 29.7 ± 0.3 μm) compared to *Spp1*$^{(+/+)}$ mice (L_m: 26.0 ± 0.3 μm). Values are mean ± standard error (n= 5 mice/strain) and statistical significance (*p<0.05) was determined by analysis of variance (ANOVA) test and all pairwise comparisons procedure (Holm-Sidak method).

Figure 5. Hierarchical clustering of altered transcripts associated with lung development in secreted phosphoprotein 1 deficient (*Spp1*$^{(-/-)}$) compared to strain matched control (*Spp1*$^{(+/+)}$) at postnatal day 14 (P14) or P28. Transcripts were significantly enriched in genes associated with lung development (n = 132 significant of 387 in the category, p = 1E-08). *Subgrouping columns*: Four major clusters were identified: (A) decreased at P14 and P28, (B) increased at P14 and decreased at P28, (C) decreased at P14 and increased at P28, or (D) increased at P14 and P28. Significant difference in transcript levels for the microarray data was analysed using ANOVA (Partek Genomics Suite, St. Louis, MO) (p<0.05). Fold change color scale is adjacent to heat map. Values are means (n = 6 – 14 mice/strain) with yellow denoting increased and purple denoting decreased in *Spp1*$^{(-/-)}$ compared to strain matched control (*Spp1*$^{(+/+)}$) mouse. Each row represents a gene and each column represents mean difference for P14 or P28

Figure 6. Transcripts associated with lung development are altered in secreted phosphoprotein 1 deficient (*Spp1*$^{(-/-)}$) as compared to strain matched control (*Spp1*$^{(+/+)}$) at postnatal day 14 (P14) or P28. (A) Lung mRNA was isolated and transcript levels determined by qRT-PCR. Values are mean ± standard error (n = 6 - 14 mice/strain) and statistical significance (*p<0.05) was determined by analysis of variance (ANOVA) test and all pairwise comparisons procedure (Holm-Sidak method). (**B**) Protein-Protein interaction network of SPP1 with proteins associated with lung development. **Abbreviations**: IGF1: insulin-like growth factor 1; WNT5A: wingless-related MMTV integration site 5A; HHIP: hedgehog interacting protein; NOTCH1: notch 1; CD44: CD44 antigen; IHH: Indian hedgehog; SHH: sonic hedgehog; HES1: hes family bHLH transcription factor 1; RUNX2: runt related transcription factor 2; RUNX3: runt related transcription factor 3; FGF2: fibroblast growth factor 2; FGFR3: fibroblast growth factor receptor 3; IGFBP1: insulin-like growth factor binding protein 1, IGFBP3: insulin-like growth factor binding protein 3; IGF2BP3:

insulin-like growth factor 2 mRNA binding protein 3; ITGAV: integrin alpha V; ITGB2: integrin beta 2; PTRC: protein tyrosine phosphatase, receptor type, C (aka CD45), CTNNB1: catenin (cadherin associated protein), beta 1; GSK3B: glycogen synthase kinase 3 beta; FZD1: frizzled class receptor 1; FZD4: frizzled class receptor 4; FZD5: frizzled class receptor 5; ROR2: receptor tyrosine kinase-like orphan receptor 2.

AJRCMB Articles in Press. Published on 09-May-2014 as 10.1165/rcmb.2013-0471OC

Figure 1:

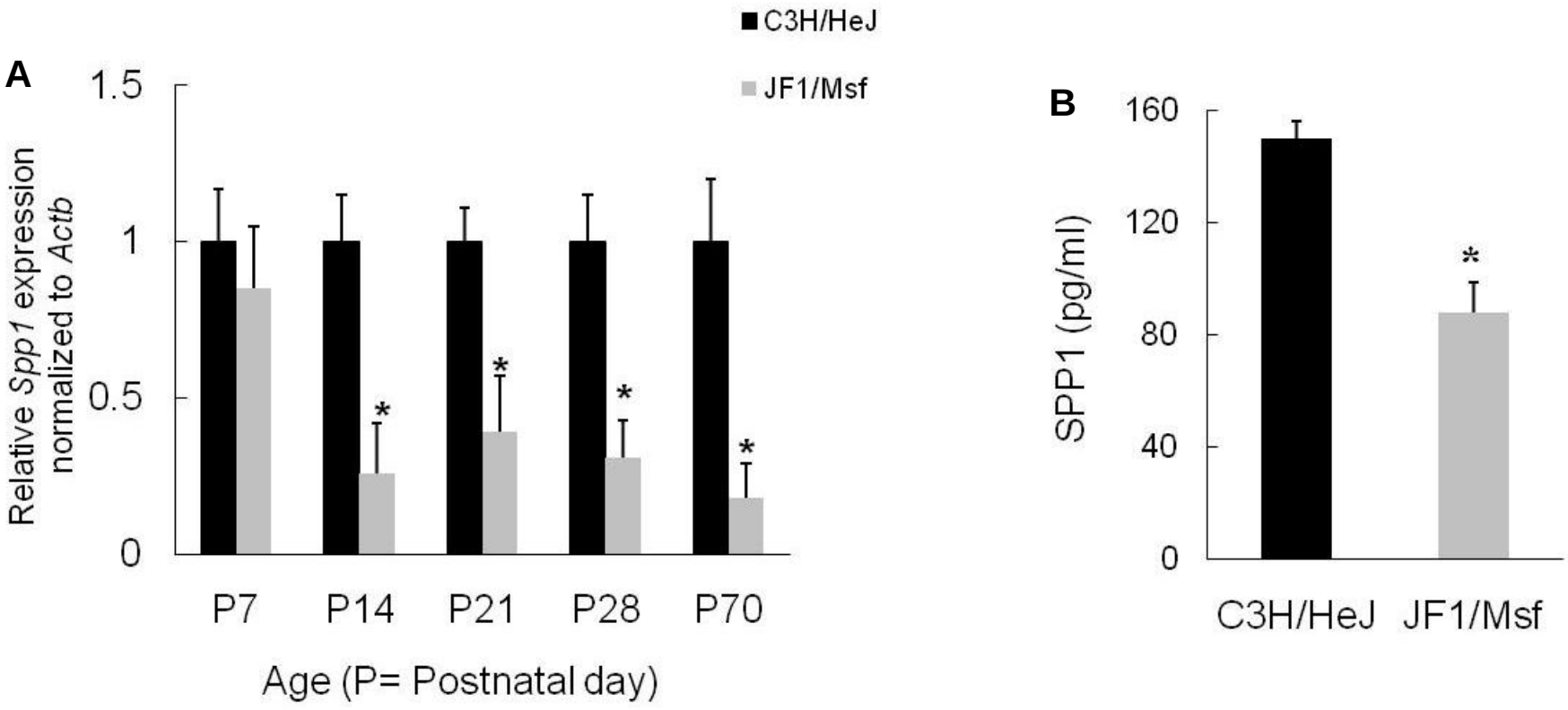

Figure 2.

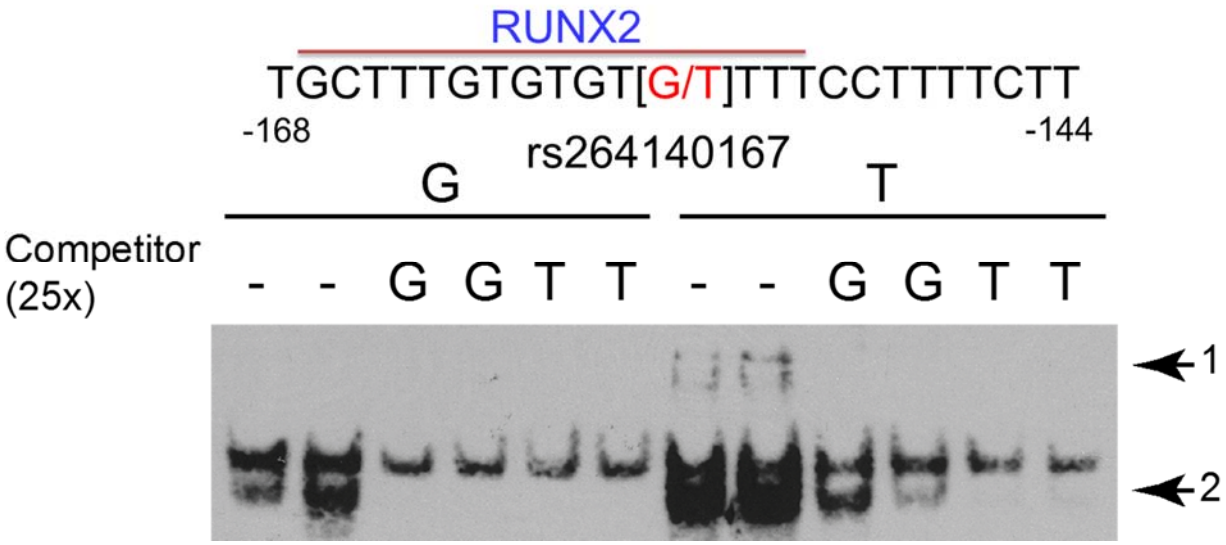

AJRCMB Articles in Press. Published on 09-May-2014 as 10.1165/rcmb.2013-0471OC

Figure 3:

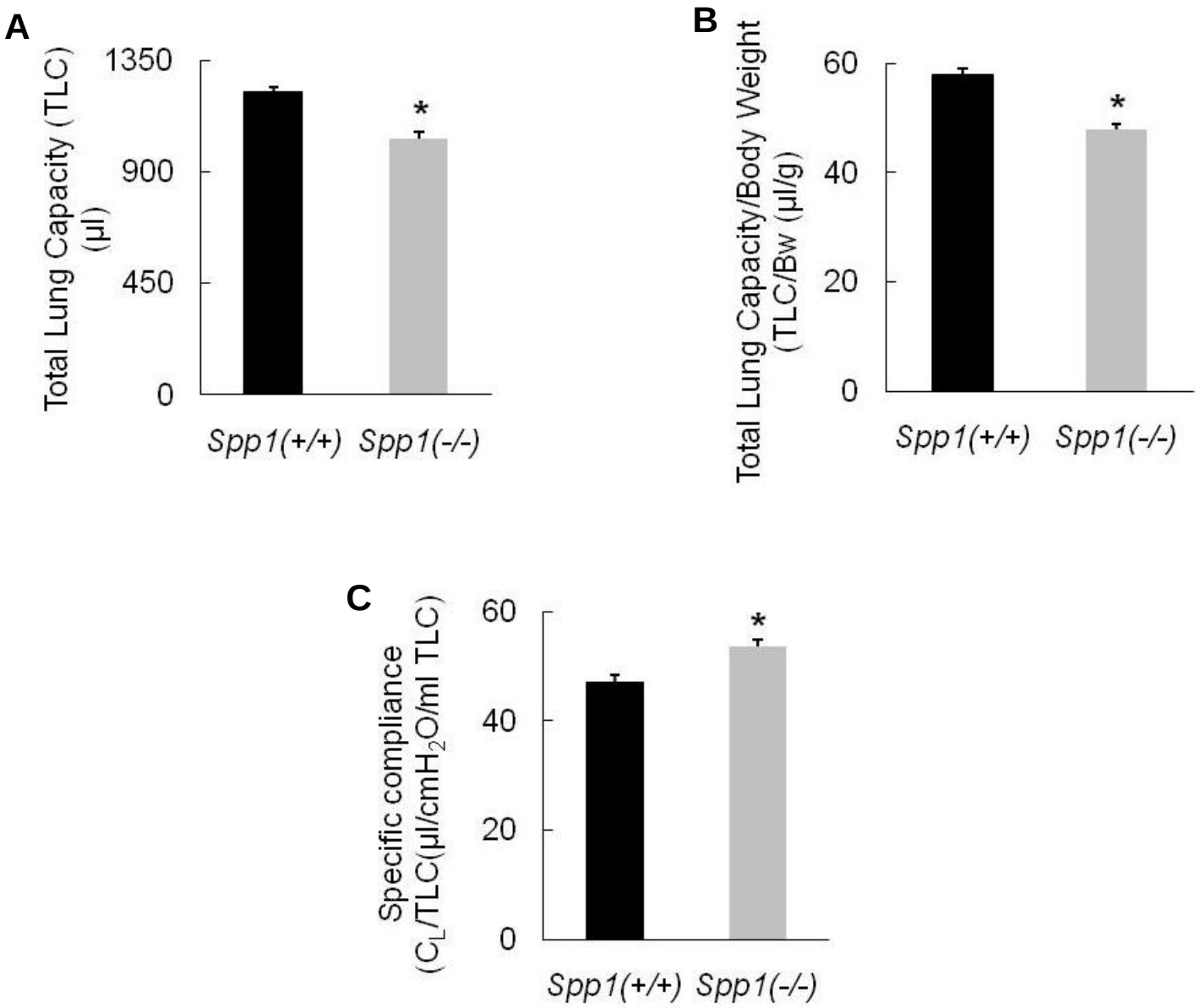

Figure 4:

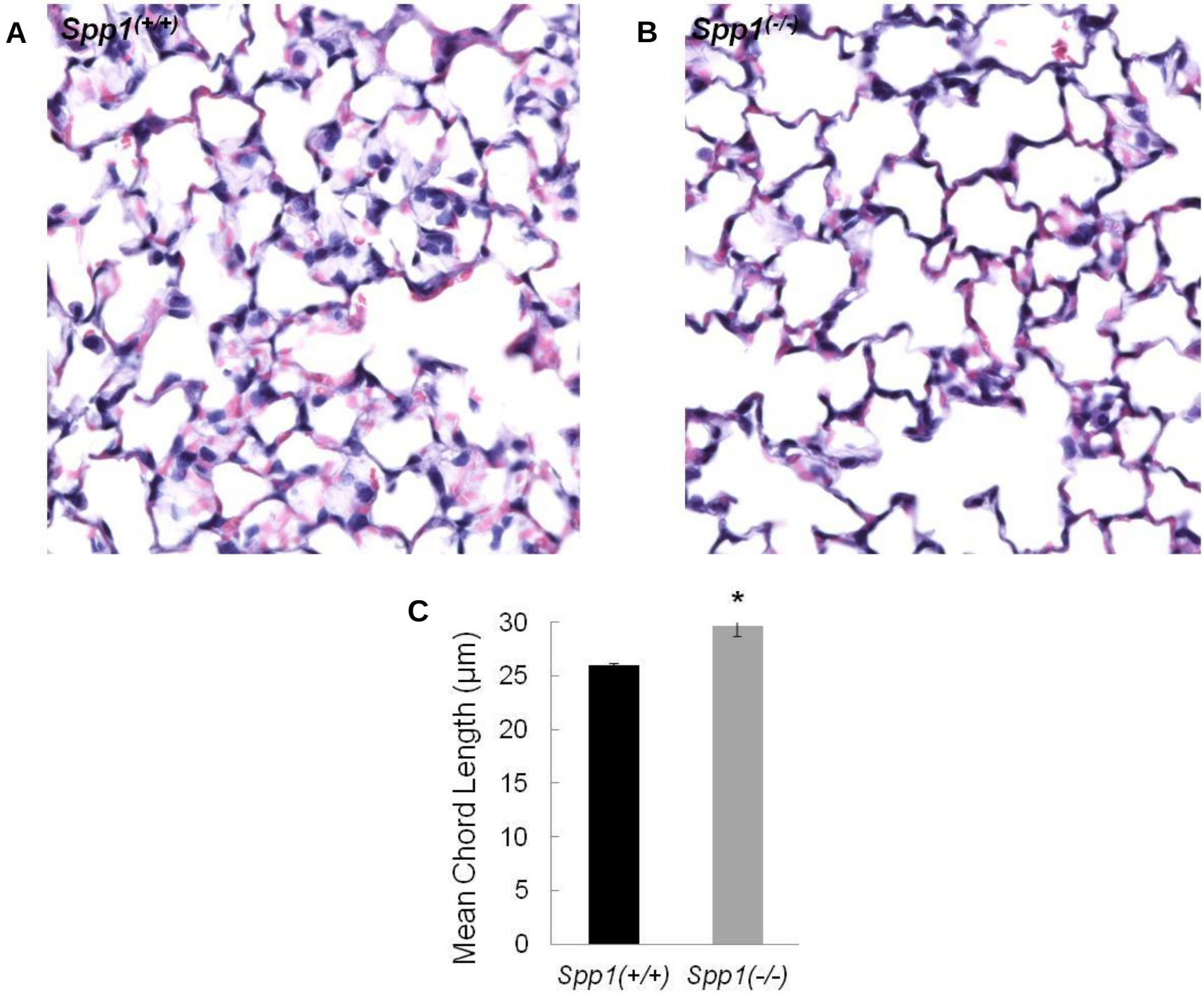

AJRCMB Articles in Press. Published on 09-May-2014 as 10.1165/rcmb.2013-0471OC

Figure 5:

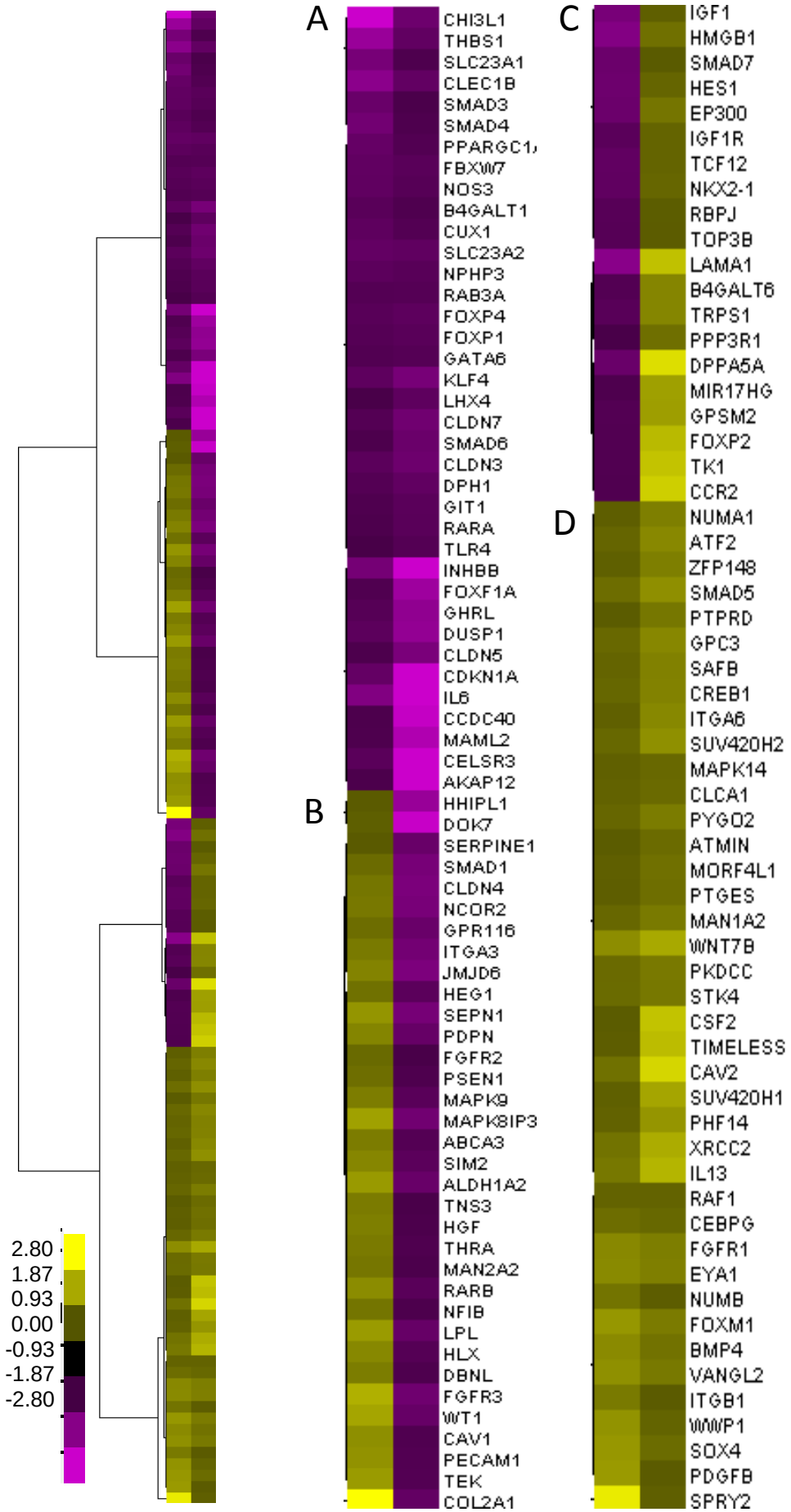

Figure 6:

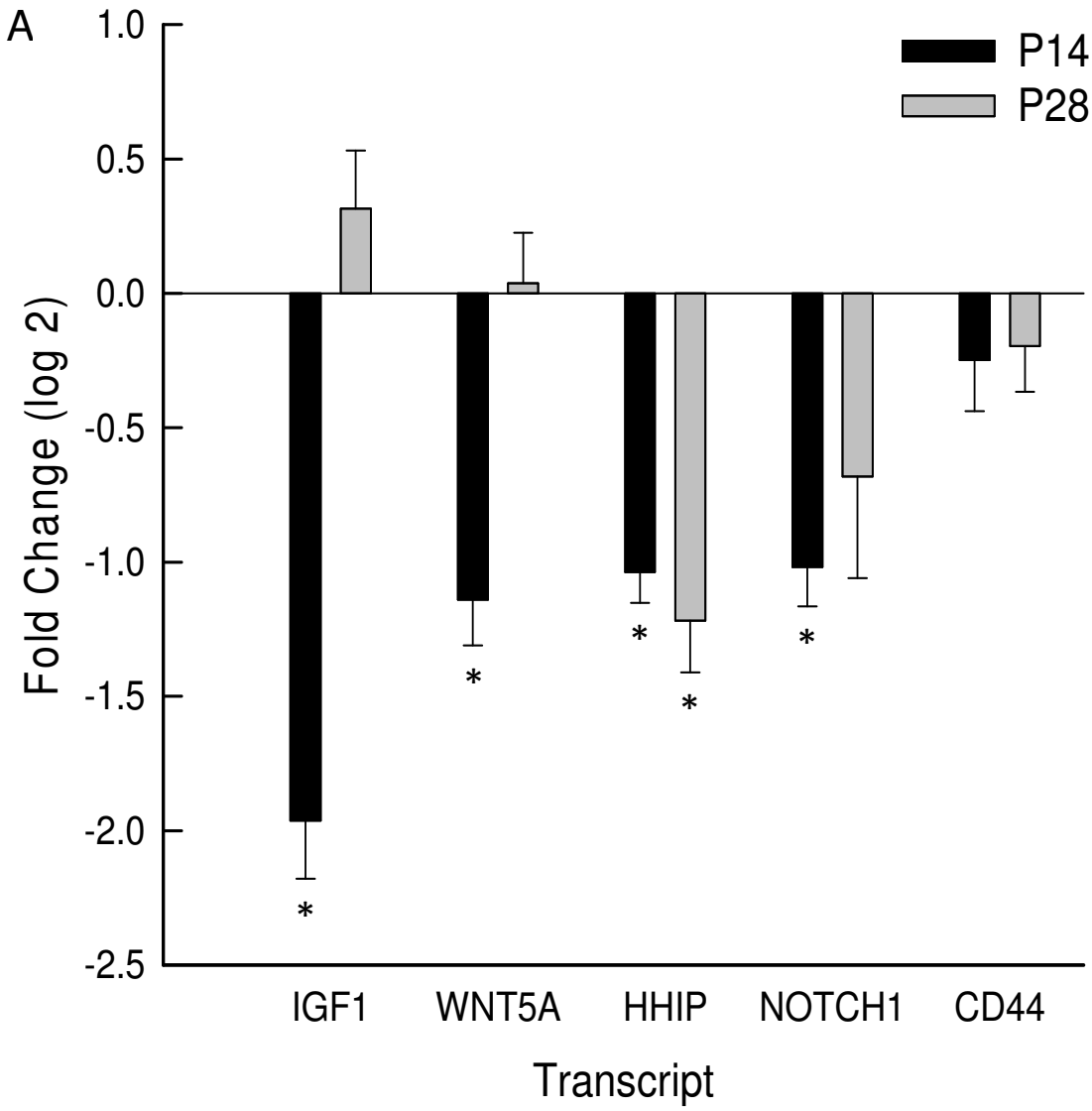

AJRCMB Articles in Press. Published on 09-May-2014 as 10.1165/rcmb.2013-0471OC

Figure 6:

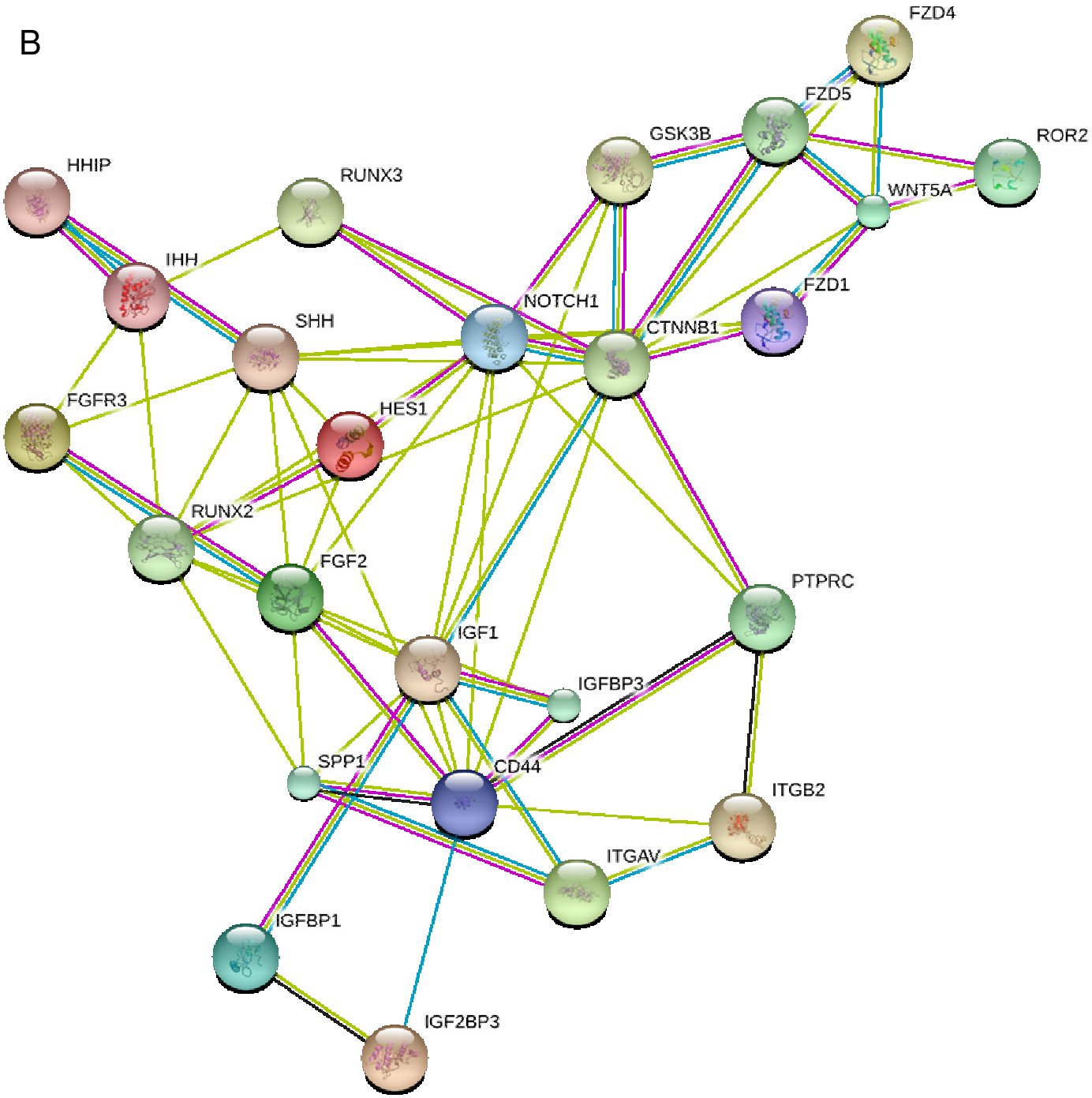

AJRCMB Articles in Press. Published on 09-May-2014 as 10.1165/rcmb.2013-0471OC

Secreted phosphoprotein 1 (*Spp1*) is a determinant of lung function development in mice

Koustav Ganguly[1,2], Timothy M. Martin[1], Vincent, J Concel[1], Swapna Upadhyay[1,3], Kiflai Bein[1], Kelly A. Brant[1], Leema George[2], Ankita Mitra[2], Tania A. Thimraj[2], James P. Fabisiak[1], Louis J Vuga[4,5], Cheryl Fattman[1], Naftali Kaminski[4,5,6], Holger Schulz[7],George D. Leikauf[1]

Supplemental Material

AJRCMB Articles in Press. Published on 09-May-2014 as 10.1165/rcmb.2013-0471OC

Detailed Materials and Methods

Animals: Mice were housed under specific-pathogen free conditions. C3H/HeJ (Cat. No. 000659), JF1/Msf (Cat. No. 003720), *Spp1*$^{(-/-)}$ [B6.129S6(Cg)-Spp1^{tm1Blh}/J, Cat. No. 004936] and *Spp1*$^{(+/+)}$ (C57BL6/J, Cat. No. 000664) mice were purchased from (Jackson Laboratory, Bar Harbor, ME). The use of animals was in accordance with the German Law of Animal Protection and approved by the Bavarian Animal Research Authority and all procedures were also approved by the IACUC of the University of Pittsburgh.

SPP1 transcript and protein analysis: Quantitative real time polymerase chain reaction (qRT-PCR) was used to determine lung SPP1 transcripts. Lungs were removed from anesthetized C3H/HeJ and JF1/Msf mice (n = 5 mice/strain/age; Postnatal days 7-70) and frozen in liquid nitrogen. Total RNA was isolated (Qiagen, Germany), quality confirmed by denaturing formaldehyde/agarose/SYBR Gold gel (Agilent Bioanalyzer Analysis), and quantified (PeqLab Nanodrop Bioanalyzer). Lung RNA (2 µg, n = 5 mice/strain/age) was reverse transcribed into cDNA (Ready-To-Go T-primed First-Strand Kit, Amersham Biosciences, Freiburg, Germany) and 1µl cDNA was used in PCR reaction solution [11.5µl Absolute qPCR SYBR Green ROX mix (ABgene, Hamburg, Germany), 1µl each primer, and 10.5µl RNAse-free water]. qRT-PCR was performed (Life Technologies 7900HT System) (15 min, 95°C; 40 cycles of 15 s, 95°C; 1 min, 60°C) using primer pairs (Sigma-Genosys, Steinheim, Germany):

SPP1*:* Forward:AGCTCAGAGGAGAAGCTT,
Reverse:CTTCAGAGGACACAGCAT;
actin, beta (ACTB) Forward:TCCATCATGAAGTGTGACGT,
Reverse: GAGCAATGATCTTGATCTTCAT.

SPP1 transcript levels were determined using the $2^{-\Delta\Delta CT}$ method and normalized to ACTB as described previously (21).

ELISA was used to determine lung SPP1 protein levels. Mice were anesthetized, lungs removed, weighed and added to 9X volume of 50 mM Tris-HCL with 2 mM EDTA, pH 7.4, lysis buffer supplemented with a protease inhibitor cocktail (Sigma-Aldrich Cat no.P8340). Following homogenisation the tissue preparation was centrifuged for 2 min in a microfuge at 13000 rpm (Eppendorf 5415R). Without disturbing the cell pellet the supernatant was aspirated. The total protein concentration in the homogenates was determined (Pierce, Rockford, IL, USA, Coomassie Plus) and ELISA (Stressgen**:** Cat. No. 900-090A) was performed.

Spp1 promoter sequencing: PCR amplification of the Spp1 promoter region was performed using genomic DNA from C3H/HeJ and JF1/Msf mice (Jackson Laboratory) performed and sequenced in forward and reverse directions (Sequiserve, Vaterstetten, Germany). The sequences of Spp1 promoter (712 bp starting -658 bp proximal to and spanning exon 1) were compared to identify single nucleotide polymorphisms (SNPs) that could affect transcription factor binding domains. The primer pairs used were as follows:

Forward: CCCAACTGACCTGGAACACAG
Reverse: CACCCTCAGAATTCAGCCAGG

Murine lung epithelial cell (MLE-15) culture and growth analysis: MLE-15 cells are an immortalized cell line obtained from lung tumors of transgenic mice containing the simian virus 40 (SV40) large T antigen under the transcriptional control of the human surfactant protein C promoter (33). They have many characteristics of alveolar type II cells, including polygonal epithelial cell morphology, microvilli, cytoplasmic multivesicular bodies, multilamellar inclusion bodies, surfactant protein B transcript expression, and phospholipid secretion. Mouse lung epithelial (MLE)-15 cells (a kind gift of Dr. Jeffrey Whitsett) (passages 22–32, 37^{o}C, 5% CO_2) were grown in RPMI 1640 medium (Invitrogen, Grand Island, NY, Cat. No. 22400-105,) containing 2 mM HEPES (Sigma, St. Louis, MO Cat. No. 90909C), 1% insulin-transferin-selenium (Invitrogen, Cat. No. 41400-045,), 10 nM hydrocortisone (Sigma, Cat. No. H-0888,), 10 nM β-estradiol (Sigma, Cat. No. E-2758), 2 mM L-glutamine (Invitrogen, Cat. No. 25030-081), 4% fetal bovine serum (Invitrogen, Cat. No. 26140-111), 100 U/ml penicillin, 100 mg/ml streptomycin (Sigma, Cat. No. P4333) (34). MLE-15 cells were seeded in 96-well culture plates at a cell density of 5×10^3 cells/well. To measure cell proliferation, subconfluent cultures were serum deprived for 24 h and 0, 1, 2 or 4 μg/ml SPP1 (R&D Systems, Inc., Minneapolis, MN Cat. No. 441-OP) was added. Growth was assessed after 48h using an alamarBlue cell viability assay (Life Technologies, Carlsbad, CA, Cat. No. DAL1025,).

Lung function measurements: Lung function measurements were performed with 12-14 wk old female *Spp1*$^{(-/-)}$ and strain, sex, and age matched control *Spp1*$^{(+/+)}$ (C57BL/6J) (n=8 mice/strain) as described previously (19, 20). Briefly, anesthetized mice were intubated and ventilated using a computer-controlled piston-type servo ventilator and concentrations of the respiratory and the test gases (He and $C^{18}O$) were measured by a magnetic sector field mass spectrometer. The volume, airway opening pressure (Pao), esophageal pressure, and gas concentration were continuously recorded and digitized for subsequent data analysis. Inspiratory reserve capacity was defined as that volume slowly inspired over 10 sec from a relaxed expiratory level to a Pao = 25 cm H_2O. Expiratory reserve volume was defined as that volume slowly expired over 10 sec from relaxed inspiratory level to Pao = -10 cm H_2O. To determine the functional reserve capacity (FRC) by the helium dilution technique, a rebreathing volume of 80% inspiratory reserve capacity containing 1% He: 21% O_2: 78%N_2 was set at a rate of 50 breaths/min for 15 cycles and the mixed He concentrations were determined by mass spectrometry. The quasi-static compliance of the pulmonary system and that of the lung was determined from the linear portion of the respective pressure–volume curve obtained during a 6 s lasting exhalation from TLC to residual volume and the C_L was derived from the transpulmonary pressure–volume curve. Series V_D was obtained using the Fowler method from single-breath wash-in measurements with 1% He in air administered for 3 s from relaxed expiratory level to TLC to slightly below FRC over 7 s without a breath-hold. D_{CO} was determined with single breath-holding method using a gas (0.3% $C^{18}O$: 1% He: 21% O_2, 71.7% N_2) started from the relaxed expiratory level to TLC over 3 s followed by a breath-holding time of 3 s and an expiration slightly below FRC. The alveolar volume (V_A) was determined according to the Cotes method. Values of lung function measurements were also normalized to body weight or lung size (e.g.,

AJRCMB Articles in Press. Published on 09-May-2014 as 10.1165/rcmb.2013-0471OC

TLC/BW, V_D/TLC).Further details of the technique including calibration and reproducibility are presented in Schulz et al. (35).

Electrophoretic mobility shift assay (EMSA): Nuclear protein extracts were obtained from MLE15 mouse lung cells [kind gift from Jeffrey Whitsett, University of Cincinnati] grown in ATCC formulated RPMI-1640 medium 30-2001 supplemented with HITES and 4% fetal bovine serum. Extracts were prepared (NEPER Nuclear and Cytoplasmic Extraction Reagents, Pierce Biotechnology, Rockford, IL), and assessed by EMSA. The binding reaction mixture containing 3.5 µg of nuclear extract, 2.25 ng of biotin-labeled polymorphic oligonucleotide probe(s), and binding buffer [in mM: 12 HEPES, pH 7.9, 4 Tris·HCl, pH 7.9, 25 KCl, 50 MgCl2, 1 EDTA, 4 dithiothreitol, 0.2 phenylmethylsulfonyl fluoride, with 100 ng/µl poly (dI-dC) and 0.05% IGEPAL CA-630] was incubated (30 min, 15°C) in a final volume of 10 µl. Double-stranded oligonucleotides were prepared by annealing complementary synthetic oligonucleotides corresponding to the *Spp1* promoter region. The nucleotide sequence of the sense strands were:

rs264140167

G-polymorphic: forward TGCTTTGTGTGTGTTTCCTTTTCTT

T-polymorphic: forward TGCTTTGTGTGTTTTTCCTTTTCTT

rs47003578

A-polymorphic: forward ATAAATGAAAAGAGTAGTTAATGAC

G-polymorphic: forward ATAAATGAAAAGGGTAGTTAATGAC

For competition assays, 25-fold excess unlabeled double-stranded variant oligonucleotides were incubated with the extracts (30 min, 23°C) before probe addition. Bound complexes were separated on 6% polyacrylamide gels and blotted onto membrane. The blot was processed with a streptavidin horseradish peroxidase conjugate-based detection method (LightShift Chemiluminescent Kit, Pierce Biotechnology). Chemiluminescence signal was detected by exposing the blot to film.

Lung morphometric analysis and immunohistochemical locationiztion: Mice were anesthetized and the lungs were fixed in situ (thorax closed) via a cannula with 10% formalin at a constant fluid pressure (25 cm H_20, 5 min). Sections (5µm thick) of paraffin-embedded, formalin fixed mouse lungs were stained with hematoxylin and eosin (AML laboratories, Rosedale, MD). Five digital images of parenchymal architecture (omitting large vascular and bronchiolar structures) from each mouse was captured at X20 magnification by an investigator blinded to the experimental groups. Images were captured from anatomically comparable regions of the lung. Mean chord length (L_m) was measured from images to estimate the alveolar size as previously descibed (23). Briefly, a series of grid lines (11 × 11 point grid) was laid over each photomicrograph to determine the number of times those lines were intercepted by alveolar tissue, with $L_m = L/L_i$, where L is the total length of the lines in the grid field and L_i is the total number of times those lines are intercepted. Chord length values the average distance between opposing walls of a single alveolus. Morphometry was performed

in 4 wk old female *Spp1*$^{(-/-)}$ mice and compared to strain, sex and age matched *Spp*$^{(+/+)}$ when the process of alveolarization is just completed during mouse lung development.

For immnunohistochemical localization, *Spp*$^{(+/+)}$ lung sections were washed with xylene and a graded alcohol series to remove paraffin. Antigen retrieval was performed by microwaving slides for 3 consecutive 5 min periods at 20% power in 1 mM citrate solution, pH 6.0. Slides were rehydrated in phosphate-buffered saline (PBS), followed by immersion in 1% H_2O_2 (10 min) to inhibit endogenous peroxidases. Slides were treated with 5% horse serum, 4% bovine serum albumin (BSA) in PBS (45 min, 20^{o}C). Primary antibody omission was used as a negative staining control. Tissue was stained using a goat anti-mouse SPP1 antibody (AF-808 R&D Systems Inc.) at 2 mg/ml in 4% BSA in PBS (1 h, 20^{o}C). Detection of SPP1 was performed using a biotinylated horse-anti-goat secondary antibody (BA-9500, Vector Laboratories Inc., Burlingame, CA) at a 1:200 dilution, a Vectastain Elite kit (PK-6100, Vector Laboratories Inc.) and aminoethylcarbazole substrate (00-2007, Invitrogen Corporation, Camarillo CA 93012 USA). Tissue was counterstained with Mayer's hematoxylin.

Microarray analysis: Lung transcript levels were measured by microarray analysis comparing postnatal day 14 (P14) *Spp1*$^{(-/-)}$ (n = 6) with P14 *Spp1*$^{(+/+)}$ (n = 14) or postnatal day 28 (P28) *Spp1*$^{(-/-)}$(n = 6) with P28 *Spp1*$^{(+/+)}$ (n = 6) female mice. Postnatal days 14 and 28 were chosen based on reduced SPP1 transcript expression pattern in JF1/Msf lungs compared to C3H/HeJ during peak phase of alveologenesis (P14) and completion of alveologenesis (P28) during mouse lung development. Lung mRNA was isolated (Trizol method), reverse transcribed, and fluorescently labeled. Each sample was hybridized to a microarray containing 31,769 murine 70-mer oligonucleotides (Aligent Technologies, Santa Clara, CA). RNA quantity was initially assessed by spectrophotometer (Life Technologies, Nanodrop ND-1000) and quality was assessed by electrophoresis (Aglient Technologies, 2100 Bioanalyzer). RNA (0.5 μg) was cyanine 3-labeled and cDNA synthesized (Aglient Technologies, RNA Spike In – One Color, 5188-5282). Labeled cRNA was transcribed from cDNA (Aglient Technologies, Quick-Amp Labeling Kit - One Color, 5190-0442,). The labeled cRNA was quantified and hybridized (65°C, 17 h) (Aglient Technologies, Gene Hybridization, 5188-5242) onto the array (Aligent Technologies, Whole Mouse Genome Kit 4x44K, G4122F). Arrays were washed and scanned (Aglient Technologies, DNA Microarray Scanner, G2505C, Feature Extraction Version 10.7.3.1).

Additional qRT-PCR: In addition 5 transcripts associated with lung development were assessed by qRT-PCR. Lung RNA (100 μg) from the P14 *Spp1*$^{(-/-)}$(n= 6) or P28 *Spp1*$^{(-/-)}$(n =6) *Spp1*$^{(-/-)}$ or P14 *Spp1*$^{(+/+)}$(n = 14) P28 *Spp1*$^{(+/+)}$ (n = 6) mice was reverse transcribed into first-strand cDNA (Life Technologies, High-Capacity cDNA Archive Reverse Transcription Kit) in a 100-μl reaction volume. cDNA (2 μl) was used in a subsequent PCR reaction using 5 μl of TaqMan® Universal PCR Master Mix (Life Technologies), 0.5 μl of each primer mixture, and 3.5 μl of RNAse-free water. Validated primer mixtures for each transcript (Life Technologies, TaqMan® Gene Expression Assays, Catalog no. 4331182: IGF1: Mm00439560_m1, WNT5A: Mm00437347_m1, HHIP: Mm00469580_m1, NOTCH1: Mm00435249_m1,CD44: Mm01277163_m1, RPL32: Mm02528467_g1) were used and results normalized to RPL32. Analysis was performed with a thermocycler

AJRCMB Articles in Press. Published on 09-May-2014 as 10.1165/rcmb.2013-0471OC

(7900HT System, Life Technology) using the following conditions: 50°C for 2 min followed by 40 cycles of 95°C for 15s and 60°C for 1 min. For relative quantification of expression of each gene between the strains, the comparative cycle number threshold (C_T) method ($\Delta\Delta C_T$) was used: $\Delta C_T = C_T$ (transcript of the gene of interest) – C_T (e.g., RPL32), and this value was calculated for each sample. The comparative $\Delta\Delta C_T$ calculation involved finding the difference between each sample's ΔC_T and the mean ΔC_T for the opposing strain at the same postnatal day. These values were converted to log 2 values with a formula in which comparative expression level= $2^{-\Delta\Delta CT}$.

Evaluation of protein-protein Interactions: To assess the possible interactions between SPP1 and the transcripts measured by qRT-PCR that are associated with lung development, an interactome was constructed using the STRING v 9.1 database (http://string-db.org/) of known and predicted associations scored and integrated, resulting in comprehensive protein networks covering >1100 organisms (S2).

Statistical Analysis: Data are presented as arithmetic mean values of n observations ± the standard error (SE). Group comparisons were performed using analysis of variance (ANOVA) and all pairwise comparisons procedure (Holm-Sidak method) (Sigma Plot 11.0 software). Significant differences ($p<0.05$) in transcript levels for the microarray data were analysed using ANOVA (Partek Genomics Suite, St. Louis, MO) and significant value corrected for multiple comparison by the Benjamini procedure (S1).

Supplemental References

S1. Benjamini Y, Hochberg Y. Controlling the false discovery rate: a practical and powerful approach to multiple testing. *J R Stat Soc B* 1995;57:289-300.

S2. Franceschini A, Szklarczyk D, Frankild S, Kuhn M, Simonovic M, Roth A, Lin J, Minguez P, Bork P, von Mering C, Jensen LJ. STRING v9.1: protein-protein interaction networks, with increased coverage and integration. *Nucleic Acids Res* 2013;41:D808-15.

Supplement Table S1. Genetic Variants in Secreted Phosphoprotein 1 Promoter

Refseq ID	Location (Basepair)*	Position Relative to Start	JF1/Msf	C3H/HeJ	C57BL/6J	Alleles
rs50363675	104434601	-510	A	A	G	G/A
rs50272366	104434628	-483	T	T	C	C/T
rs255180990	104434679	-432	[-]	[-]	[CTGCCG]	[-/CTGCCG]
rs33370718	104434790	-321	C	T	T	T/C
rs229736737	104434804	-307	C	C	C	C/G
rs33389579	104434819	-292	T	T	T	G/T
rs46562537	104434823	-288	C	C	C	C/T
rs33725711	104434826	-285	A	A	A	A/G
rs219162996	104434852	-259	C	C	C	[-/C]
rs50725813	104434898	-213	T	C	T	T/G
rs47003578	104434913	-198	G	A	G	A/G
rs47530358	104434914	-197	G	G	G	A/G
rs264140167	104434953	-158	G	T	G	G/T
rs225456020	104434968	-143	TTT	[-]	[-]	[-/T]
rs234069704	104434981	-130	[-]	TTTTTTTTTTA	[-]	[-TTTTTTTTTTA]
Start Site	104435111	0				
rs48302365	104435117	6	C	C	C	A/C

*Location is position on mouse chromosome 5.

Supplemental Figure S1. Alignment of the secreted phosphoprotein 1 promoter sequence in the C57BL/6J, C3H/HeJ, and JF1/Msf mouse strains. DNA from C3H/HeJ and JF1/ Msf was polymerase chain reaction amplified and sequenced. Sequences were then aligned to the reference C57BL/6J mouse strain. Single nucleotide polymorphisms are indicated in red.

	-500	-490	-480	-470	-460	-450	-440	-430	-420	-410
C57BL/6J	GGAGTACAAA	ACAGAGCCAC	TGTGGCCCGG	CCAACCTAAG	CTACCGAATA	CAAAGGCAAA	AGGGAGGGTC	TGAAAGTTCT	GCCGAGACAG	CAGTTTTCTA
C3H/HeJ	GGAGTACAAA	ACAGAGCCAC	TGTGGCTCGG	CCAACCTAAG	CTACCGAATA	CAAAGGCAAA	AGGGAGGGTC	TGAAAGTT--	----AGACAG	CAGTTTTCTA
JF1/Msf	GGAGTACAAA	ACAGAGCCAC	TGTGGCTCGG	CCAACCTAAG	CTACCGAATA	CAAAGGCAAA	AGGGAGGGTC	TGAAAGTT--	----AGACAG	CAGTTTTCTA
	-400	-390	-380	-370	-360	-350	-340	-330	-320	-310
C57BL/6J	GATTTAAGTA	AGTCTGAGAG	AATCAAATTG	TGTATCCATG	TGGCCTTTAT	CTGTAACTTA	GATAGGAGAA	TCCATACCTT	TCATCCCCAT	TGATGTTTT
C3H/HeJ	GATTTAAGTA	AGTCTGAGAG	AATCAAATTG	TGTATCCATG	TGGCCTTTAT	CTGTAACTTA	GATAGGAGAA	TCCATACCTT	TCATCCCCAT	TGATGTTTT
JF1/Msf	GATTTAAGTA	AGTCTGAGAG	AATCAAATTG	TGTATCCATG	TGGCCTTTAT	CTGTAACTTA	GATAGGAGAA	TCCATACCTC	TCATCCCCAT	TGATGTTTT
	-300	-290	-280	-270	-260	-250	-240	-230	-220	-210
C57BL/6J	TCTACTAATT	CAGTAACTAT	AAACAAAGTC	TCTGTGAGGG	TGATCTACTC	ATGGATCCCT	GATGCTCTTC	CGGGATTCTA	AATGCAGTCT	ATAAATGAAA
C3H/HeJ	TCTACTAATT	CAGTAACTAT	AAACAAAGTC	TCTGTGAGGG	TGATCTACTC	ATGGATCCCT	GATGCTCTTC	CGGGATTCTA	AATGCAGCCT	ATAAATGAAA
JF1/Msf	TCTACTAATT	CAGTAACTAT	AAACAAAGTC	TCTGTGAGGG	TGATCTACTC	ATGGATCCCT	GATGCTCTTC	CGGGATTCTA	AATGCAGTCT	ATAAATGAAA
	-200	-190	-180	-170	-160	-150	-140	-130	-120	-110
C57BL/6J	AGGGTAGTTA	ATGACATCGT	TCATCAGTAA	TGCTTTGTGT	GTGTTTCCTT	TTCTTCC- - -/TTT	TTTTTTTTTT	T----------ACCACAAAA	CCAGAGGAGG	AAGTGTAGGA
C3H/HeJ	AGAGTAGTTA	ATGACATCGT	TCATCAGTAA	TGCTTTGTGT	GTTTTTCCTT	TTCTTCC- - -/TTT	TTTTTTTTTT	TTTTTTTTTTACCACAAAA	CCAGAGGAGG	AAGTGTAGGA
JF1/Msf	AGGGTAGTTA	ATGACATCGT	TCATCAGTAA	TGCTTTGTGT	GTGTTTCCTT	TTCTTCCTTTTTT	TTTTTTTTTT	T----------ACCACAAAA	CCAGAGGAGG	AAGTGTAGGA
	-100	-90	-80	-70	-60	-50	-40	-30	-20	-10
C57BL/6J	GCAGGTGGGC	CGGGTAGTGG	CAAAAACCTC	ATGACACATC	ACTCCACCTC	CTGATTGGTG	GAGACTGTCT	GGACCAGCAT	TTAAATTCTG	GGAGGTCTG
C3H/HeJ	GCAGGTGGGC	CGGGTAGTGG	CAAAAACCTC	ATGACACATC	ACTCCACCTC	CTGATTGGTG	GAGACTGTCT	GGACCAGCAT	TTAAATTCTG	GGAGGTCTG
JF1/Msf	GCAGGTGGGC	CGGGTAGTGG	CAAAAACCTC	ATGACACATC	ACTCCACCTC	CTGATTGGTG	GAGACTGTCT	GGACCAGCAT	TTAAATTCTG	GGAGGTCTG

AJRCMB Articles in Press. Published on 09-May-2014 as 10.1165/rcmb.2013-0471OC

Supplemental Figure S2. Electrophoretic mobility shift assay (EMSA) analysis of SNP rs47003578 (-198 nucleotides from the transcription start site) in the *Spp1* promoter revealed no specific nuclear protein-target DNA binding capacity. EMSA of nuclear protein extract prepared from mouse lung epithelial cells (MLE-15) and 25-mer probes (-186bp to -210bp from the start site) containing the G or A allele in the middle of the biotinylated oligonucleotide. The signal detected represented background as it was not competed by non-labeled oligonucleotide containing the G or A allele.

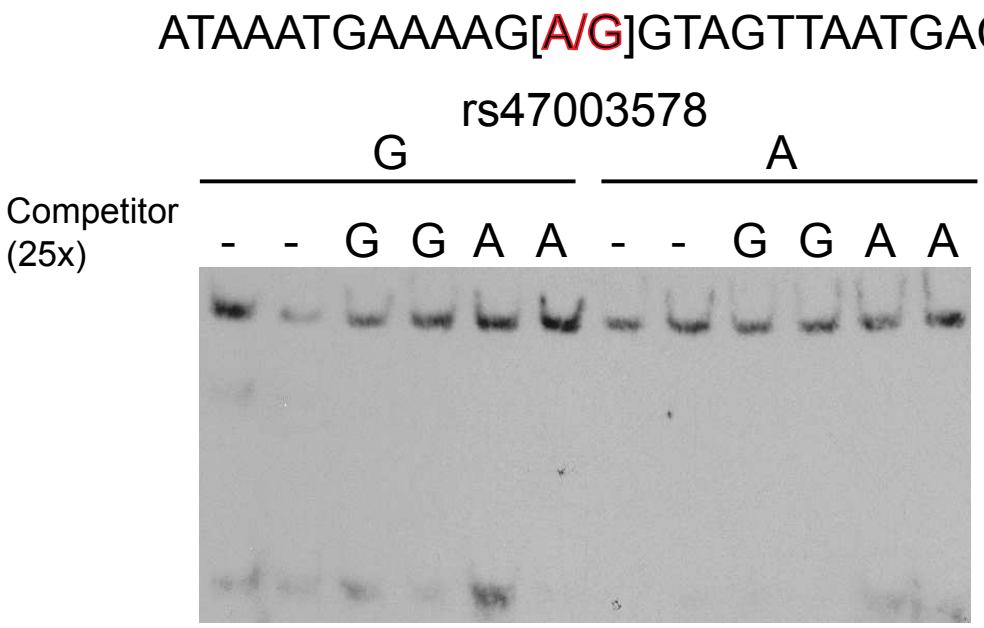

Supplemental Figure S3. Secreted phosphoprotein 1 (SPP1) induces growth of type II-like pneumocytes. Increasing concentrations of SPP1 (0, 1.0, 2.0, and 4.0 μg/ml) produced dose dependent growth of MLE-15 cells as measured by alamarBlue assay. Values are mean ± standard error (n=6 experiments) and statistical significance (*p<0.005) was determined by analysis of variance (ANOVA) test and all pairwise comparisons procedure (Holm-Sidak method).

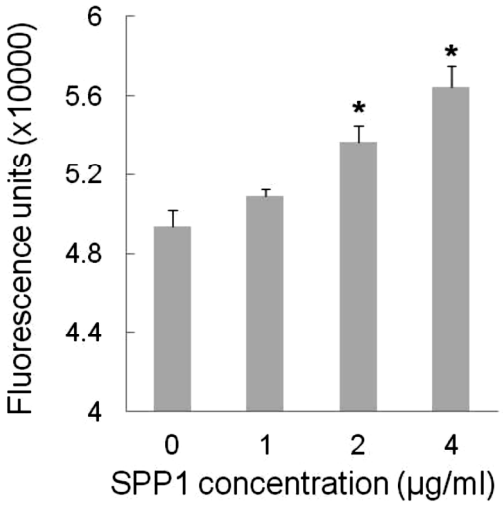

AJRCMB Articles in Press. Published on 09-May-2014 as 10.1165/rcmb.2013-0471OC

Supplemental Figure S4. Localization of secreted phosphoprotein 1 (SPP1) in the lungs of C57BL/6J mice. SPP1 immunostaining was detected in the bronchial epithelial cells, matrix of airway, alveolar type II cells, and alveolar parenchyma (B: male; C: female). A: Section incubated without primary antisera. Magnification: 10X; Inset: 40X.

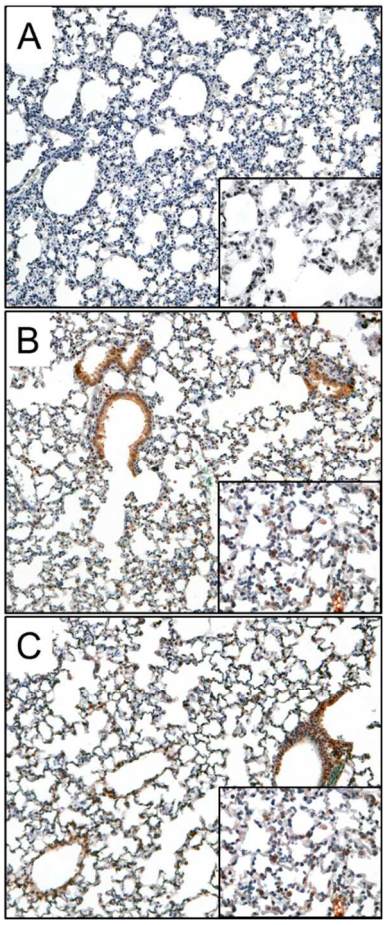

Supplemental Figure S5. Alignment of the secreted phosphoprotein 1 (*SPP1*) promoter sequence from human and mouse genomic sequence. Top Panels: Human *SPP1* and mouse *Spp1* sequence of the 5' untranslated promoter region proximal to the transcriptional start site. The runt related transcription factor 2 (RUNX2) binding sites are indicated by bold letters. The RUNX2 sites underlined indicate the human rs11439060 G insertion at -156 bp and the mouse rs264140167 G to T conversion at -158 single nucleotide polymorphism (variants marked in red). The AACCA site is near the rs234069704 TTTTTTTTTA insertion at -130 bp that provides a RUNX2 binding site present in C3H/HeJ mouse strain, which is not present in the JF1/Msf or C57BL/6J mouse strains. **Lower Panel:** Alignment of this region demonstrates 84% conversation between human and mouse.

Human (-211 to -1 bp from *SPP1* transcription start site)

TTAATGATATTGTACATAAGTAATGTTTTAACTGTAGATTGTGTGTGTGCGTTT**TT**[G/GG]**TT**TTTTTT
TGTTTT**AACCAC**AAAACCAGAGGGGGAAGTGTGGGAGCAGGTGGGCTGGGCAGTGGCAGAAAACCTCATG
ACACAATCTCTCCGCCTCCCTGTGTTGGTGGAGGATGTCTGCAGCAGCATTTAAATTCTGGGAGGGCTTG
GTTGT

Mouse (-200 to -1 bp from *Spp1* transcription start site)

TTAATGACATCGTTCATCAGTAAT**GCTTTGTGTGT**[G/T]**TTT**CCTTTTCTTCCTTTTTTTTTTTTTT**AA**
CCACAAAACCAGAGGAGGAAGTGTAGGAGCAGGTGGGCCGGGTAGTGGCAAAAACCTCATGACACATCAC
TCCACCTCCTGATTGGTGGAGACTGTCTGGACCAGCATTTAAATTCTGGGAGGTCTGAGCCACC

Alignment of 5' proximal promoter region in human and mouse (84% conversed)

```
Human       TTAATGATATTGTACATAAGTAATGTTTTAACTGTAGATTGTGTGTGTGCGttttG--t
            ||||||| || || ||| ||||||| |||          ||||||| | | ||| |   |
Mouse       TTAATGACATCGTTCATCAGTAATGCTTTG---------TGTGTGTTTCCTTTTCTTCCt

Human       ttttttttgttttAACCACAAAACCAGAGGGGGAAGTGTGGGAGCAGGTGGGCTGGGCAG
            |||||||| |||||||||||||||||||| |||||||| |||||||||||| ||| ||
Mouse       TTTTTTTTTTTTTAACCACAAAACCAGAGGAGGAAGTGTAGGAGCAGGTGGGCCGGGTAG

Human       TGGCAGAAAACCTCATGACACAATCTCTCCGCCTCCCTGTGTTGGTGGAGGATGTCTGCA
            ||||| ||||||||||||||| ||| |||| ||| ||||  |||||||||  |||||| |
Mouse       TGGCA-AAAACCTCATGACAC-ATCACTCCACCT-CCTG-ATTGGTGGAGACTGTCTGGA

Human       GCAGCATTTAAATTCTGGGAGGGCTTGGTTGTC
             |||||||||||||||||||| ||  |    |
Mouse       CCAGCATTTAAATTCTGGGAGGTCTGAGCCACC
```